Notch-IGF1 signalling in biliary epithelial cells drives their expansion and inhibits hepatocyte differentiation

Title: Notch-IGF1 signalling in biliary epithelial cells drives their expansion and inhibits hepatocyte differentiation

Authors: Sarah E. Minnis-Lyons[1], Sofía Ferreira- González[1], Niya Aleksieva[1], Tak Yung Man[1], Victoria Gadd [1], Michael J. Williams [1], Rachel V. Guest [2], Wei-Yu Lu[3], Benjamin J. Dwyer[1], Tam Jamieson [4], Colin Nixon[4], Noemi Van Hul [5], Frederic P. Lemaigre [6], John McCafferty J[7], Isabelle Leclercq[8], Owen J Sansom [4,9], Luke Boulter[10, #,†], Stuart J Forbes[1,#,†]

[#]Corresponding Authors:

Prof Stuart Forbes (stuart.forbes@ed.ac.uk), Centre for Regenerative Medicine, Edinburgh, UK

Dr Luke Boulter (luke.boulter@ed.ac.uk), MRC Human Genetics Unit, Edinburgh, UK

Affiliation:

1. Centre for Regenerative Medicine, Scottish Centre for Regenerative Medicine, Edinburgh, UK.
2. Clinical Surgery, Royal Infirmary of Edinburgh and University of Edinburgh, Edinburgh, UK.
3. Centre for Liver and Gastrointestinal Research, Institute of Immunology and Immunotherapy, University of Birmingham, Birmingham, UK
4. Institute of Cancer Sciences, University of Glasgow, Garscube Estate, Glasgow, UK
5. Department of Biosciences and Nutrition, Karolinska Institutet, Huddinge, Sweden.
6. Université catholique de Louvain, de Duve Institute, Brussels, Belgium.
7. IONTAS Ltd., Iconix Park, London Road, Pampisford, Cambridgeshire, United Kingdom.
8. Laboratory of Gastroenterology, Université Catholique de Louvain, Brussels, Belgium
9. Cancer Research UK Beatson Institute, Garscube Estate, Switchback Road, Glasgow, UK.
10. MRC Human Genetics Unit, Institute of Genetics and Molecular Medicine, Edinburgh, UK

[†]Joint senior authorship

One sentence summary: During liver injury, Notch signaling in Biliary Epithelial Cells facilitates IGF1 to drive proliferation and inhibit their differentiation into hepatocytes.

Declaration: The authors have no conflicts of interest to declare.

Abstract: The adult liver contains a population of facultative progenitor cells (known variously as Oval Cells, Hepatic Progenitor Cells, HPCs, or proliferating Biliary Epithelial Cells, BECs) which, following injury, proliferate and differentiate into hepatocytes, thereby restoring liver function. Although previous studies have shown that Notch signalling is essential for bile duct formation from these cells, it has not been determined whether Notch signalling is required for BECs to replenish hepatocytes following injury in the mammalian liver. This limitation is largely due to the mammalian models used to study hepatic repair from BECs, which rely on chronic damage and continual proliferation of BECs. In this study, we use a strict model of hepatic repair where large-scale hepatocyte injury and regeneration is initiated through the acute loss of *Mdm2* in hepatocytes. This results in a rapid, coordinated proliferation of BECs allowing us to dissect the role of Notch signalling in this process. We find that transient, early activation of Notch signalling and entrance into cell cycle precedes the phenotypic expansion of BECs. Notch1 and Notch3 mediate this process and accordingly Notch inhibition results in the reduction of BEC proliferation. This decrease in BEC number results in a failure of BECs to differentiate into hepatocytes, indicating that Notch-dependent expansion of BECs is essential for hepatocyte regeneration. Finally, we found that Notch signalling regulates insulin-like growth factor-1 receptor (IGF1R) levels and show that activation or inhibition of IGFR1 signalling regulates BEC number. Critically, increasing BEC number (by activating IGFR signalling) suppresses the differentiation of BECs into hepatocytes, suggesting that BEC expansion has different signalling mechanisms to hepatocyte differentiation.

Introduction:

Following injury, the adult liver is able to regenerate from a population of facultative Biliary Epithelial Cells (BECs) that proliferate and differentiate into hepatocytes in response to injury, thereby reconstituting damaged epithelial cells and restoring normal liver function(1, 2). Throughout regeneration, a cellular and acellular microenvironment surrounds BECs (also known as Hepatic Progenitor Cells, HPCs or Oval Cells) (3) and provides a number of developmental signals(4–7). These signals are responsible for maintaining a balance between BEC proliferation and differentiation, thereby ensuring that regeneration is sufficient, collectively, in human disease, BECs and this microenvironment are termed the ductular reaction (8). BECs are able to differentiate into two epithelial lineages, cholangiocytes that make up the bile duct, a tubular network that drains bile form the liver into the bowel and hepatocytes, which comprise the metabolically active parenchyma of the liver. Following bile duct injury, we and others have shown that Notch signalling is necessary for BECs to reconstitute the bile duct

and as such Notch signaling is considered a master-regulator of the ductular lineage(9, 10). Whether Notch signalling is required for BECs to regenerate hepatocytes following hepatic injury in the mammalian liver is not clear, although recent data from a number of studies in the Zebrafish, suggests that Notch signalling maintains BECs in a naïve state and that BECs can differentiate when the suppressive effects of Notch signalling are removed (11–13). These data from the fish suggest that contrary to evidence in mouse, Notch signaling does function in the replenishment of hepatocytes after injury. A limitation of previous murine studies investigating the signals that govern the proliferation and differentiation of BECs into hepatocytes, is that the majority of murine models rely on establishing chronic hepatic injury. This results in a continuous activation, proliferation and differentiation of BECs. Therefore in these models, BECs are at various stages of their lifecycle, making it difficult to resolve the signals that govern the various states of proliferation and differentiation(14–16).

To overcome this, we used a model where largescale, liver-wide injury is induced by the acute genetic loss of *Mdm2* in hepatocytes(2, 17). In this model, hepatocytes become senescent(18) and as a result BECs undergo coordinated activation and proliferation ultimately differentiating to reconstitute hepatocytes. Using this approach, we have been able to resolve in a temporal way the role of Notch signalling during hepatocyte regeneration from BECs and we describe how Notch signalling is activated prior to the overt expansion of BECs in the liver. In this model of acute hepatocyte *Mdm2*-loss we have found that Notch signalling promotes BEC proliferation by modulating the levels of IGF1R, thereby sensitising BECs to IGF1. Through modulating this Notch-IGF1R pathway in vivo, using a combination of animal models (both of acute hepatocyte *Mdm2*-loss as well as classical dietary-induced injury models, MCD and CDE, where hepatocytes have been shown to arise from the differentiation of BECs or HPCs(2, 19)) we have found that the numbers of BECs can be altered. Importantly, suppression of BEC proliferation results in a failure of BECs to differentiate into hepatocytes indicating that in hepatic regeneration a sufficient number of BECs must be generated before differentiation can occur. To our surprise, we also found that increasing BEC number through IGF1 signalling inhibits differentiation, leading us to conclude that there is a fine balance between BEC generation and their differentiation into hepatocytes, that must be satisfied for repair from BECs to occur.

Results:

Notch signalling is activated early in BECs following hepatic injury. The Notch signalling pathway is essential for the formation of bile ducts from embryonic hepatoblasts(20, 21) and is reactivated in adult bile duct regeneration where it directs BECs into a cholangiocyte lineage(9, 22, 23), therefore we sought to address whether Notch also regulates hepatocyte regeneration from BECs. We have previously described a mouse model of hepatic regeneration where large numbers of hepatocytes can be generated from BECs (2, 17). Known as the Ah-Cre::Mdm2$^{fl/fl}$ mouse, this model relies on the specific expression of Cre recombinase in hepatocytes following administration of β-napthoflavone, which activates the *Cyp1a1* promotor to drive Cre expression. In these mice, both alleles of *Mdm2* are also flanked by LoxP sites; as a result, following Cre activity *Mdm2* is excised resulting in the stabilisation of TRP53 and upregulation of *p21* in hepatocytes. In this model, large scale hepatocyte senescence (driven by p21 upregulation), results in liver injury (Supplementary Figure 1A), hepatocyte apoptosis (Supplementary Figure 1B) and BEC proliferation and differentiation in order to reconstitute the liver parenchyma(2, 17). As liver regeneration is initiated at a single time point (when β-napthoflavone is administered) it is possible to track the temporal dynamics of BECs as they proliferate prior to their differentiation into hepatocytes.

Following *Mdm2*-loss in Ah-Cre::Mdm2$^{fl/fl}$ mice, the number of panCK positive BECs begins to increase throughout the liver within 5-7 days following induction and by 14 days following induction, there are significantly higher numbers of panCK-positive BECs that invade into the parenchyma compared to mice that still have intact *Mdm2* (Figure 1A). These cells are also positive for the BEC marker, SOX9 (Supplementary Figure 1C). Given the rapid increase in BECs following hepatic injury, we hypothesised that biliary epithelial cells would continuously proliferate to generate large numbers of daughter cells in order to replenish lost hepatocytes; therefore we stained *Mdm2*-deleted livers for KI67, a marker of proliferation.

Contrary to what we expected, the proportion of proliferating BECs is high early-on (between days 3-5) following initiation of injury, when we begin to see the emergence of BECs, however this is not maintained throughout regeneration and after 5 days, the proportion of BECs in the cell cycle decreases (Figure 1B). As Notch signaling is mitogenic in other progenitor cell systems(24, 25) and is required for bile duct regeneration (9, 10), we evaluated whether components of the Notch signalling pathway are expressed during hepatocyte repair. Following initiation of injury, there is a rapid increase in the mRNA expression of Notch receptors, *Notch1* and

Notch3 (Figure 1C) between days 3-5 of regeneration but not *Notch2* (Supplementary Figure 1D) and Notch ligands, *Jagged1* and *Jagged2* (Figure 1D). *Dll1* was the only other Notch ligand detectable and this did not change throughout the time course (Supplementary Figure 1D). To verify that the Notch signalling pathway is activated in proliferating BECs, used a transgenic mouse line, CBF::H2B^{Venus} that reports active Notch signalling with single cell resolution(26) and crossed this into our AhCre::Mdm2$^{fl/fl}$ line, such that we could identify cells that have active Notch signaling during hepatocyte regeneration (known as AhCre::Mdm2$^{fl/fl}$::CBF^{H2BVenus}). We found that proliferating BECs were strongly positive for the Venus (eYFP) in the early phase (day 5) following hepatocyte *Mdm2* recombination (Figure 1E), suggesting that in line with the expression of Notch receptors, this signaling pathway is also active. The transcriptional expression of Notch pathway components is reduced at later time points, having peaked at 3-5 days following hepatocyte *Mdm2*-loss. To validate independently that the Notch pathway is activated in BECs, we stained liver tissue from mice with hepatocyte *Mdm2*-deletion for Notch pathway components and found that NOTCH1 and NOTCH3 proteins are expressed by BECs at day 3 and day 5, respectively. Furthermore, NOTCH1 intracellular domain localises to the nucleus of BECs reiterating that the Notch-1 receptor is cleaved and the pathway is activated (Figure 1F, single stains available in Supplementary Figure 5). Previous work in ductular regeneration has shown that the Notch ligand, JAGGED1 is expressed by myofibroblasts surrounding proliferating ducts (9), however during hepatocyte regeneration from BECs, we could find little evidence indicating Notch ligands are expressed by fibroblasts or macrophages, rather JAGGED1 is expressed by the BECs themselves (Figure 1G).

Inhibition of Notch signalling impairs BEC proliferation and hepatocyte differentiation. Whilst the expression of Notch pathway components correlates with an increased number of BECs entering the cell cycle, it is not clear whether Notch signalling drives proliferation of BECs *per se*. To determine whether this is the case, we induced *Mdm2*-loss in hepatocytes to induce BEC proliferation and gave a pharmacological inhibitor of Notch signalling, DAPT, that prevents the activity of γ-secretase, thereby preventing Notch receptor cleavage (from hereon-in known as Notch-i). As our model relies on a single genetic insult to initiate injury and hepatocyte regeneration, we were able to inhibit Notch signalling either early during regeneration or later in this process (Figure 2A). When we administered Notch-i early during regeneration (between days 2 and 4 following injury), the point where the Notch signalling is highly activated, the number of BECs that were proliferative and the total number of panCK positive BECs was significantly reduced (Figure 2B). When Notch-i was administered late, at a point

where *Notch1* and *Notch3* mRNA levels are lower (at 7-10 days following injury), the number of proliferative BECs remained the same, demonstrating that Notch signalling only drives BEC proliferation in the early phases of hepatocyte repair (Figure 2B and 2C). Given that inhibition of γ-secretase can influence a number of cleaved cell surface proteins along with Notch-receptors, we sought to verify that NOTCH1 and NOTCH3 specifically regulate BEC proliferation. Following hepatocyte *Mdm2*-loss and the activation of BECs, we inhibited NOTCH1 and NOTCH2 receptors using receptor specific inhibitory antibodies (administered 1 day following *Mdm2*-loss) or NOTCH3 through genetic deletion using a *Notch3*$^{-/-}$ mutant mouse line. Inhibition of NOTCH1 and deletion of NOTCH3 significantly reduced the number of proliferative BECs and the total number of panCK-positive BECs following injury *in vivo* (Figure 2D) and are associated with a significant reduction in BEC proliferation and mRNA expression of Notch pathway target genes *in vitro* (Supplementary Figure 2A -2F). Inhibition of the Notch signalling pathway (either with DAPT, blocking antibodies or through receptor deletion) and reduction in BEC numbers did not appear to make liver injury worse (as determined by ALT levels, Supplementary Figure 2G-J). However, in the context of NOTCH1 inhibition or genetic NOTCH3 deletion (where BEC proliferation is reduced) we found that the levels of serum Bilirubin are significantly decreased, suggesting that the formation of a ductular reaction, in these models at least, contributes to cholestasis (Supplementary Figure 2K and 2L).

Recent work has suggested that BECs differentiate into hepatocytes and that these differentiated cells then undergo proliferation to reconstitute the parenchyma(27). To determine whether inhibition of Notch signalling and reduced BEC numbers affected hepatocyte differentiation, we utilized an Osteopontin driven CreERT^2 (OPN-iCRE^{ERT2}::R26R^{eYFP}) to irreversibly label BECs and their progeny with eYFP such that we can monitor the differentiation of BECs into hepatocytes (19). In the healthy adult mouse liver, OPN- iCRE^{ERT2} only labels BECs. In injury, however, hepatocytes have also been shown to upregulate OPN, therefore to ensure we did not capture any other cells and that we only labelled BECs we dosed animals with tamoxifen and then left them for a 2-week "wash-out" prior to initiating injury(28). Hepatocyte injury was induced by feeding OPN-iCRE^{ERT2}::R26R^{eYFP} mice a Choline Deficient, Ethionine Supplemented diet, CDE (Figure 2E), and the proportion of hepatocytes labelled with eYFP (Figure 2F) is significantly higher than in uninjured livers (Figure 2G), as previously described(19). Following Notch-i in these OPN-iCRE^{ERT2}::R26R^{eYFP}, CDE-fed mice, however, the number of proliferative eYFP+ BECs is reduced (Supplementary Figure 3A, left panel) as too are the number of lineage traced hepatocytes (Figure 2F and 2G). We also confirmed that in a second dietary model of hepatocyte injury, the Methionine-

Choline Deficient (2), MCD model that Notch-i consistently reduces the number of proliferating BECs (Supplementary Figure 3A, right panel) demonstrating that BECs proliferation driven by Notch signaling is not restricted to the CDE model. Collectively, our data indicate that Notch-dependent BEC proliferation is essential for normal hepatocyte reconstitution from a BEC origin.

Notch signalling regulates the expresson of IGF1R by BECs. Notch signalling is involved in the expansion of progenitor cell pools in a range of developmental and adult tissues(29–31). It is widely accepted, however, that Notch does this by supressing differentiation and maintaining progneitor cells in a state that is receptive to mitogenic signals(32, 33). In Alagille syndrome, loss of Notch signalling due to mutations in *Jagged1* results in the dysregulation of IGF1 signalling(34) therefore we sought to determine whether Notch signalling can regulate IGF1 signalling in adult BECs and define whether IGF1 induces BECs to proliferate.

Following deletion of *Mdm2* in hepatocytes and initiation of hepatic regeneration from BECs, both IGF1 and its activated receptor, pIGF1R^{Y1161} are expressed by BECs in vivo (Figure 3A) and throughout the timecourse following *Mdm2*-inactivation, the mRNA expression of *Igf1r*, maps closely with the expression of the Notch pathway target gene, *HeyL* (Supplementary Figure 3B). In vitro, the BEC cell line, BMOL produce their own IGF1, which they secrete into the media (Figure 3B). Following treatment with Notch-i *in vitro*, BMOLs do not reduce their expression of *Igf1* at the mRNA level (Supplementary Figure 3C), rather the levels of *Igf1r* transcript (Figure 3C) and IGF1R protein (Figure 3D and Supplementary Figure 3D) are significantly decreased, suggesting that Notch inhibition can regulate signalling through the IGF1 pathway through modulation of the IGF1 receptor levels *in vitro*. Finally, consistent with this, we measued the transcript levels of both *Igf1* and *Igf1r* in mice that had received Notch-i for three days during early hepatocyte regeneration (following *Mdm2*-deletion in the Ah-Cre::Mdm2$^{fl/fl}$ line) when *Notch1* and *Notch3* are most highly expressed (Figure 2A) and found that expression of *Igf1r* mRNA, but not that of *Igf1* was significantly reduced (Figure 3E). Furthermore, in these Ah-Cre::Mdm2$^{fl/fl}$ mice undergoing hepatcoyte regeneration, when treated with Notch-I the expression of pIGF1R^{Y1161} is reduced, whereas in vehicle treated animals, pIGF1R^{Y1161} is expressed and localises to the plasma membrane of BECs (Figure 3F).

Signalling through the IGF1-receptor directly regulates BEC proliferation: Having identified that Notch signalling can regulate the expression of IGF1R in BECs and given that IGF1-IGF1R signalling is a potent mitogen for other cell types, we sought to address whether signalling through IGF1R promotes the proliferation of BECs. *In vitro*,

BECs treated with the IGF1R inhibitor AG1024, reduced their proliferation in a dose dependant manner (Supplementary Figure 4A), indicating that IGF1-IGF1R signalling is mitogenic in BECs. *In vivo*, IGF1R is expressed by a number of different cell types(35), therefore, to better undertand the role of IGF1 signalling in hepatic regeneration, we conditionally deleted *Igf1r* (using *Igf1r*^{flox} mice) in BECs using the OPN-CreER^{T2} transgenic mouse line, whilst concurrently labelling them with eYFP (known as OPN-CreER^{T2}::IGF1$^{fl/fl}$::R26R^{eYFP} mice) (Figure 3G) and inducing liver injury by feeding mice a hepatotoxic CDE diet. Following CDE-induced hepatic injury, OPN-CreER^{T2}::IGF1$^{fl/fl}$::R26R^{eYFP} mice, which lack *Igf1r* in their BECs failed to amount a proliferative BEC response as determined through a reduced number of eYFP positive BECs, similarly the number of eYFP-positive BECs entering cell cycle was also significantly reduced (Figure 3H). Given that IGF1-IGF1R signalling is a potent activator of the AKT/mTOR signalling pathway, we verified that phospho-mTOR was expressed by proliferating BECs in Ah-Cre::Mdm2$^{fl/fl}$ mice folloing *Mdm2*-deletion (Supplementary Figure 4B) and then inhibited this by treating Ah-Cre::Mdm2$^{fl/fl}$ mice undergoing BEC-mediated hepatcoyte regeneration with Rapamycin. In Rapamycin treated mice we found fewer proliferating BECs *in vivo* compared to vehicle treated animals (Supplementary Figure 4C and 4D), suggesting that mTOR can promote BEC proliferation.

<u>Therapeutic modulation of BEC number with IGF1 does not result in increased hepatocyte regeneration:</u> One of the ultimate aims of regenerative medicine is to identify small molecules that can alter the regenerative response and improve tissue repair. A core tenant of many therapies is that increasing the pool of endogenous stem or progenitor cells will ultimately improve the regenerative output of the tissue. Whether this is actually true in BEC mediated liver regeneration, however, has not been determined.

Our data indicates that therapeutic modulation of Notch-IGF1 signalling could affect BEC number and ultimately alter how many hepatocytes are replenished following injury. As BEC number undergoes rapid expansion from day 5 following hepatocyte *Mdm2*-loss, and that this is the point at which *Igf1r* mRNA is most highly expressed, we treated Ah-Cre::Mdm2$^{fl/fl}$ mice with either AG1024 (known as IGF1R-i) to reduce signalling through IGF1R or recombinant IGF1 (rIGF1), to stimulate IGF1R activation 6-9 days following hepatocyte *Mdm2*-loss. Following treatment with IGF1R-i, the number of proliferating BECs is reduced, as is the total number of BECs throughout the liver, indicating that BECs respond to IGF1 signalling levels during hepatocyte regeneration (Figure 4A and 4B). Conversely, treatment with rIGF1, significantly increases the number of BECs that enter cell cycle compared

to animals that received control treatment and the overall number of BECs within the liver is increased (though this does not reach statistical significance) (Figure 4C and 4D).

Having determined that modulation of IGF1R through either therapeutic inhibition or activation can directly affect the number of BECs that are proliferative in the Ah-Cre::Mdm2$^{fl/fl}$ model following hepatic injury, we sought to determine whether increasing the pool of BECs in the liver would increase the number of BEC derived hepatocytes. To do this, we utilised a previously published model of regeneration where hepatocyte senescence is induced in the liver of Krt19Cre^{ERT}::R26^{tdTomato} transgenic mice by expressing p21 in hepatocytes (using an AAV8:TBG-p21, an adeno associated virus that is highly specific for hepatocytes) and injuring the liver using the hepatotoxic MCD diet (2). Recent work has shown that, in the context of injury, the Krt19Cre^{ERT} mouse does not have ectopic activation of the Cre transgene in hepatocytes (28) and so represents the most robust tool for genetically labelling and lineage tracing BECs in order to assess BEC to hepatocyte differentiation, particularly when the number of hepatocytes arising from BECs could be limited. As previous studies have shown that following the withdrawal of MCD-induced injury, hepatocytes can be lineage traced from K19-positive BECs (by staining for tdTomato) in this mouse line, we administered rIGF1 or vehicle alone to this model to determine whether stimulating IGF1R results in the formation of more lineage traced hepatocytes (Figure 4E). Following rIGF1 treatment, the number of proliferating BECs and total number of BECs within the livers of rIGF1 treated mice was increased at the end of this study (Figure 4F), reiterating that supplementing rIGF1 is able to increase BEC number in a range of murine models of hepatocyte regeneration. Finally, we stained and quantified tissue for lineage traced (tdTomato-positive), HNF4α-positive hepatocytes. Interestingly, we found that there was a significant reduction in tdTomato positive hepatocytes lineage traced from BECs (Figure 4G and 4H), indicating that increasing BEC number alone is insufficient to increase BEC to hepatocyte differentiation (summarised in Figure 4I).

Together, our data show that the Notch signalling pathway is necessary for the proliferation of BECs destined to become hepatocytes and that Notch does this by promoting BECs to become sensitive to signalling through IGF1R, yet other factors are necessary to promote the differentiation of these cells into hepatocytes.

Discussion:

The role of Notch signalling in bile duct development is well described(20, 34, 36) and recent work has shown that these developmental signalling pathways are reactivated in the adult when bile ducts are injured(9, 10). However, early data from us and others indicated that there was not a role for Notch signalling in hepatic regeneration; Biliary Epithelial Cells that were destined for hepatocyte differentiation had Notch pathway components transcriptionally down regulated and Notch's function was suppressed in BECs through the expression of the E3-ligase, *Numb*(9, 12). Previous mammalian models of hepatic regeneration promoted BEC proliferation and differentiation(16). In these models, progenitor cells were continually generated; undergoing proliferation and differentiation at different rates, therefore identifying pathways that regulated BEC proliferation and differentiation in the mammalian liver has been difficult, though data form zebrafish has suggested that Notch signaling is required for BEC to hepatocyte differentiation(12, 13). Recent advances in mammalian models of liver regeneration, however, have provided new tools to answer fundamental questions about BEC biology(2). These types of models, where a single, timed insult results in the proliferation and differentiation of BECs into hepatocytes have been discussed elsewhere(37, 38), however they allow, for the first time, temporal resolution of the signalling pathways involved in hepatocyte regeneration from a progenitor cell. Single cell RNA (scRNA) sequencing from regenerating adult livers has found that the Yap signalling pathway is critically important for BEC proliferation. These studies have indicated that Yap signalling, through the upregulation of Notch, could promote the proliferation of BECs. Whether this is a direct action of Notch acting as a mitogen or whether Notch signalling allows BECs to become sensitised to other mitogenic signals was not investigated(6, 7).

We hypothesised that Notch signalling sits at the centre of a signalling network (potentially regulated by Yap signalling) which then maintains BECs in a state permissive to proliferation. Here, we show that two Notch receptors (*Notch1* and *Notch3*) are increased in a temporally restricted manner. *Notch2* (which has an essential role in bile duct development during embryogenesis) does not change overtime and *Notch4* was undetectable (Supplementary Figure 1D). In our model, activation of Notch1 or Notch3 signalling promotes the proliferation of BECs. However, specific inhibition or genetic deletion of these single receptors is sufficient to reduce the number of BECs in cell cycle, suggesting that signalling through Notch1 and Notch3 is not redundant and indicating that Notch1 and Notch3 might play different roles in the activation and subsequent proliferation of BECs. Of note, we found that in our model of large scale hepatocyte regeneration (using the AhCre::Mdm2$^{fl/fl}$

line) that the proliferation of BECs precedes hepatocyte apoptosis. The proliferation of BECs has previously been associated with the formation of an inflammatory microenvironment(39–41) and indeed signalling from immune cells to BECs has been shown to initiate the formation of the ductular reaction(42, 43). At a tissue level, this temporal separation of BEC proliferation and differentiation, and the apoptosis of hepatocytes makes sense as the number of BECs-derived hepatocytes needs to be sufficicent to maintain liver function prior to the clearance of injured hepatocytes. However, what maintains this balance in regeneration is poorly defined.

What is clear from our studies is that Notch signalling increases the sensitivity of BECs to stimulation with IGF1, through positivity regulating IGF1R signalling in BECs. Inhibiting Notch signalling or inhibiting signalling through the IGF1R axis, is sufficient to reduce the number of BECs cells in cycle. This has interesting implications for both liver cancer, which appears to rely on the activation of developmental signalling pathways, including Notch(44, 45), and also in regenerative medicine, where relatively few therapeutically tractable signalling pathways have been identified that can increase the number of progenitor cells within a regenerating system. In this study, we identify IGF1 as one such factor, which increases the number of proliferating BECs and has the potential to improve progenitor-mediated regeneration. In our work in animal models of hepatocyte regeneration from BECs, however, we found that expansion of BECs was insufficient to regenerate more hepatocytes, instead, we found that increasing the number of BECs suppressed hepatocyte differentiation compared to control animals. The relationship between proliferation and differentiation in stem/progenitor systems is complex and requires the integration of a number of pro-proliferative factors (such as cyclin dependent kinases) with pro-lineage regulators (such as transcription factors). How these two states are reconciled in hepatic regeneration is not known, however recent work investigating the epigenetic landscape in BEC mediated liver regeneration could start to unpick the relationship between these two fundamental cellular states(46, 47). We cannot discount another outcome of course, that IGF1R signalling can directly suppress BEC-to-Hepatocyte differentiation, and further work is needed to understand this, particularly given the biphasic role of Notch in BEC differentiation in zebrafish models of hepatocyte regeneration(11, 12).

This work highlights the importance of Notch-IGF1 signalling in hepatocyte regeneration and rather than being a strict signal, positioning BECs into the cholangiocyte lineage, Notch acts as a common signal to expand progenitor cells prior to their differentiation. Furthermore, these data suggest that increasing the number of

BECs in patients with hepatic injury maybe insufficient to promote regeneration, additional therapies that drive expansion and differentiation would be required.

Materials and Methods:

Animal studies: AhCre MDM2 strains: AhCre::MDM2$^{fl/fl}$ were crossed with Notch3^{d1} (Notch3$^{-/-}$) to give AhCre::MDM2$^{fl/fl}$::Notch3$^{+/+}$, AhCre::MDM2$^{fl/fl}$::Notch3$^{-/-}$ strains. AhCre::MDM2$^{fl/fl}$ were also crossed with CBF-H2B^{Venus} transgenic Notch reporter mice to give AhCre::Mdm2fl/fl::CBF^{H2BVenus}. OPN-iCreER^{T2}::R26R^{YFP} mice were crossed with Notch3$^{-/-}$ as above to give OPN-iCreER^{T2}::R26R^{YFP}::Notch3$^{+/+}$ and OPN- CreER^{T2}::R26R^{YFP}::Notch3$^{-/-}$, and Igf1r$^{fl/fl}$ (Jackson Laboratories stock number 012252) to give OPN-iCreER^{T2}::R26R^{YFP}::Igf1r$^{fl/fl}$ and OPN-iCreER^{T2}::R26R^{YFP}::Igf1r$^{wt/wt}$.

All AhCre MDM2$^{fl/fl}$ strains received 20mg/kg beta-naphthoflavone (BNF) (Sigma-Aldrich) in corn oil intra-peritoneal (i.p.) for Cre induction. For Notch inhibition experiments mice received 50mg/kg/dose DAPT (N-[N-(3,5-Difluorophenacetyl)-L-alanyl]-S-phenylglycine t-butyl ester) (Sigma-Aldrich) or equivalent volume of vehicle daily for 3 days by i.p. injection. Notch1 (clone: aN1_E7 or aN1_E10) or Notch2 (clone: aN2_B6 or aN2_B9) blocking antibody or control antibody was administered by single dose of 10mg/kg by i.p. injection 24 hours after Cre-induction. AhCre::MDM2$^{fl/fl}$::Notch3$^{+/+}$ and AhCre::MDM2$^{fl/fl}$::Notch3$^{-/-}$ mice received only BNF induction. Mice in experiments receiving inhibitors or agonists of the IGF1-mTOR axis received daily i.p. injection of: AG1024 (Santa Cruz Biotechnology) 30ug/dose or vehicle, rapamycin (Sigma-Aldrich) 10mg/kg/dose or vehicle or recombinant murine IGF1 (rIGF1) (Sigma-Aldrich) 0.5mg/dose or vehicle. OPN-iCreER^{T2}::R26R^{YFP} mice received the CDE-stop protocol (choline-deficient ethionine-supplemented diet, MP Biomedicals) as previously described, commencing Cre-induction with tamoxifen at 21 days and injury diet at least 14 days after final tamoxifen dose when the mice reached 20g. During the 2 week 'STOP' period DAPT (25mg/kg) or equivalent volume of vehicle was administered three times per week by i.p. injection. OPN-iCreER^{T2}::R26R^{YFP} strains OPN-iCreER^{T2}::R26R^{YFP}::Notch3$^{+/+}$, OPN-iCreER^{T2}::R26R^{YFP}::Notch3$^{-/-}$, OPN-iCreER^{T2}::R26R^{YFP}::Igf1r$^{fl/fl}$ and OPN-iCreER^{T2}::R26R^{YFP}::Igf1r$^{wt/wt}$ having been generated through crosses with mice on a C57/Bl6 background.

To determine whether IGF1 affects the formation of lineage traced hepatocytes (Figure 4), a mixture of males and female 8-12 week old Keratin19-CreERT::R26R^{tdTomato} mice were used.

The Keratin19-CreERT::R26R^{tdTomato} mice were induced by 3 individual i.p. injections of Tamoxifen (20mg/ml, *Sigma*) at the dose of 4mg. Mice received two weeks of normal diet after the last Tamoxifen injection. 5 x 10^{11}

viral AAV8.TBG.p21 (Addgene) particles were reconstituted in 100µL and injected intravenously through tail vein injection with Ultra-Fine Insulin Syringes (*BD*). Mice receive one more week of normal diet before starting Methionine and Choline Deficient (MCD) diet (MP Biomedicals) for 14 days followed by four days of normal diet. Then the mice received two intraperitoneal daily doses of recombinant murine-IGF1 (Peprotech, prepared at 0.05 mg per dose in 100 ul of sterile saline) or saline control during four consecutive days followed by four additional days of recovery on normal diet. In our lineage tracing study, one animal of the saline group did not have a tdTomato expression and was therefore excluded from the analysis of the tdTomato+ hepatocytes.

All animal experiments were conducted in accordance to the UK Home Office PPL awarded to Prof Stuart Forbes. All mice were genotyped by Transnetyx (Memphis, TN, USA) and were maintained in 12h light/dark cycles on a predominantly C67Bl6/J genetic background.

Cell culture: The BEC cell line BMOL was maintained in WilliamsE medium containing 2% foetal calf serum (FCS) (Life Technologies). Cells were tested for the presence of mycoplasma in-house at the beginning of the study and were found to be negative. For in vitro cell viability assays, cells were plated at $2x10^5/cm^2$ density and treated for 48 hours with DAPT or AG1024 or the relevant vehicle at the concentrations detailed in the figures. Anti-Notch antibodies or control were used at 10µg/ml. MTT assay was conducted using 3-(4,5-dimethylthiazol-2-yl)-2,5-diphenyltetrazolium bromide (5mg/ml) (Sigma-Aldrich) diluted in PBS (Sigma-Aldrich). Cells were treated for 12 hours, and MTT crystals were dissolved in DMSO and read at 570/690nm using a FluoStar Omega (BMG Labtech). EdU incorporation assay (ThermoFisher Scientific) was conducted as described in the manufacturer's instructions after 24-hour treatment of cells with DAPT (10µM), or volume-matched DMSO.

Immunohistochemistry: At sacrifice, livers were perfused with 5mls sterile PBS into the IVC before fixation overnight in 10% buffered formaldehyde. After paraffin embedding, tissue sections were cut at 4 µm. After de-waxing sections were subject to heat-mediated antigen retrieval followed by blocks to peroxide (Vector), avidin/biotin (Life technologies) where appropriate prior to protein block (Vector). Sections were incubated overnight with primary antibodies at 4°C. After washing, sections were stained with species-appropriate secondary antibodies conjugated to Alexa 488, Alexa 555 (Life technologies), or Biotin (Vector). For colorimetric stains, sections were incubated with ABC reagent (Vector) and developed using DAB (Vector) before

counterstaining with Harris Haematoxylin and Scott's tap water. For a complete list of primary antibodies, see Supplementary Table1.

Microscopy and cell counting: Images were obtained on a Nikon Eclipse E600 microscope. Cell counts were performed manually using Fiji ImageJ (EMBL) on blinded slides and more than 20 consecutive non-overlapping fields at x200 (colorimetric) or x400 (immunofluorescent) magnification. Interlobular bile ducts were excluded from quantification. Picrosirius red quantification was performed on 30 consecutive non-overlapping x200 fields by pixel analysis using Adobe Photoshop CS6.

For analysis of PCNA positivity in RFP or YFP-expressing cells after performing immunofluorescent staining for the fluorescent reporter, PCNA and DAPI, slides were scanned using the Operetta high-content analysis system (PerkinElmer). A minimum of 30 10X long working distance objective fields (0.4cm^2) liver tissue was analyzed using the Columbus image data storage and analysis system. Briefly, a sliding parabola was applied to the DAPI channel to remove variation in background level across and between samples. All nuclei were identified using method M standard settings and from this population, cells positive for the reporter were identified based on a common threshold. From this second population those with nuclear PCNA staining were again identified using a common threshold. Results are reported as % RFP or YFP positive cells also PCNA positive. Fields containing artefacts that affected image analysis were excluded manually.

Quantification of the percentage of biliary-derived hepatocytes (Figure 4) was done in a semi-automated manner. 35 non-overlapping images (x20 magnification) were acquired per mouse using Operetta High Content Imaging System (Perkin Elmer). Total cell count (DAPI-positive nuclei) and total hepatocyte count (HNF4α-positive nuclei) were quantified in an automated manner using a segmentation strategy and Columbus image analysis software (Perkin Elmer). Biliary-derived hepatocytes were quantified manually, identified by the co-localisation of DAPI and HNF4α in the nucleus and tdTomato-positive cytoplasm.

Real-time PCR and gene expression analysis: Cells and tissues were lysed into Tri-Reagent (Ambion) and homogenized. Lysates were mixed with 1:5 chloroform/TriReagent and the aqueous phase containing RNA was collected. Cells were lysed directly into RLT lysis buffer (Qiagen). RNA was precipitated with isopropanol. The

precipitate was applied to an RNeasy Mini column (Qiagen) according to the manufacturer's protocol. Isolated RNA was quantified using a NanoDrop 1000, and 1µg was reverse transcribed using the Quantitect RT kit (Qiagen) as per the manufacturer's instructions. q-rtPCR was performed using SYBR green master mix (Qiagen) and Quantitect primers (Qiagen) (See Supplemental Table for complete primer list). Data were analysed using the LightCycler system and normalized to the housekeeping gene *Gapdh*. All samples were run in triplicate.

Elisa detection of IGF1 Conditioned medium from BMOL cells for 48 hours was tested for IGF1 concentration using an IGF1 Mouse ELISA kit (Abcam ab100695) following the manufacturer's protocol. A standard curve was generated using protein standards within the kit and absorbance of this and test samples were read using a spectophotometer (SPECTROstar Omega). This was normalised to protein content of secreting cells (determined using a BSA standard and Pierce reagent) as a surrogate for cell number.

Serum analysis: Serum analysis used commercial kits according to the manufacturer's instructions; serum albumin (Alb), bilirubin and alanine transaminase (ALT) (Alpha Laboratories); aspartate aminotransferase (AST) and alkaline phosphatase(ALP) (Randox laboratories); Cholesterol (Wako Chemicals GmbH). All kits were adapted for use on a Cobas Fara centrifugal analyser (Roche Diagnostics).

Immunoblotting: Cells extracts were prepared from BMOL cells treated with DAPT (10µM) or vehicle for 48 hours. Protein content was quantified using a BSA standard and Pierce reagent before being resolved using SDS-PAGE. Immunoblots were incubated at 4°C overnight with primary antibody rabbit anti-Igf1R^{Y1161} (Abcam) or anti-beta-actin clone AC-74 (Sigma-Aldrich). Appropriate horseradish peroxidase labelled secondary antibodies were used (Cell Signaling Technologies) and signal detected with ECL reagent (Thermo Scientific).

Statistical analysis: Prism software (GraphPad Software version 8) was used for all statistical analysis. Data are presented as mean ± s.e.m. n refers to biological replicates. Normal distribution of data was determined using the D'Agostino and Pearson omnibus normality test. For parametric data, data significance was analysed using a two-tailed unpaired Student's t-test. In cases where more than two groups were being compared, then a one-way ANOVA was used. In instances where the n was too small to determine normal distribution or the data were

non-parametric then a two-tailed Mann–Whitney U-test was used. Kruskall-Wallis test was used when comparing multiple non-parametric data.

Normal distribution was determined by Shapiro-Wilk test. The data was normally distributed and statistical significance was determined using unpaired *t*-test. Statistical significance was assumed at $p < 0.05$. Data is presented as mean ± standard error of the mean (SEM).

Study approval: All studies involving human tissue were approved by the University of Edinburgh and NHS Lothian Academic and Clinical Central Office for Research Development (ACCORD) tissue governance unit.

Supplementary Material:

Supplementary Figure 1: Deletion of Mdm2 in hepatocytes induced apoptosis and induces BECs to proliferate

Supplementary Figure 2: In vitro inhibition of Notch signalling reduces BEC proliferation.

Supplementary Figure 3: Supplementary Figure 3: Notch signalling regulates IGF1 sensitivity by regulating IGF1R activity

Supplementary Figure 4: mTOR signalling can control BEC proliferation following hepatic injury.

Supplementary Figure 5: Single channel images of immunohistochemical staining in this manuscript.

Supplementary Table 1: Antibodies and Primers used in this study.

References:

1. Huch, M., H. Gehart, R. Van Boxtel, K. Hamer, F. Blokzijl, M. M. A. Verstegen, E. Ellis, M. Van Wenum, S. A. Fuchs, J. De Ligt, M. Van De Wetering, N. Sasaki, S. J. Boers, H. Kemperman, J. De Jonge, J. N. M. Ijzermans, E. E. S. Nieuwenhuis, R. Hoekstra, S. Strom, R. R. G. Vries, L. J. W. Van Der Laan, E. Cuppen, and H. Clevers. 2015. Long-term culture of genome-stable bipotent stem cells from adult human liver. *Cell* 160: 299–312.

2. Raven, A., W. Y. Lu, T. Y. Man, S. Ferreira-Gonzalez, E. O'Duibhir, B. J. Dwyer, J. P. Thomson, R. R. Meehan, R. Bogorad, V. Koteliansky, Y. Kotelevtsev, C. Ffrench-Constant, L. Boulter, and S. J. Forbes. 2017. Cholangiocytes act as facultative liver stem cells during impaired hepatocyte regeneration. *Nature* 547: 350–354.

3. Lorenzini, S., T. G. Bird, L. Boulter, C. Bellamy, K. Samuel, R. Aucott, E. Clayton, P. Andreone, M. Bernardi, M. Golding, M. R. Alison, J. P. Iredale, and S. J. Forbes. 2010. Characterisation of a stereotypical cellular and extracellular adult liver progenitor cell niche in rodents and diseased human liver. *Gut* 59: 645–654.

4. Van Hul, N., N. Lanthier, R. Espaol Suer, J. Abarca Quinones, N. Van Rooijen, and I. Leclercq. 2011. Kupffer cells influence parenchymal invasion and phenotypic orientation, but not the proliferation, of liver progenitor cells in a murine model of liver injury. *Am. J. Pathol.* 179: 1839–1850.

5. Jung, Y., K. D. Brown, R. P. Witek, A. Omenetti, L. Yang, M. Vandongen, R. J. Milton, I. N. Hines, R. A. Rippe, L. Spahr, L. Rubbia-Brandt, and A. M. Diehl. 2008. Accumulation of Hedgehog-Responsive Progenitors Parallels Alcoholic Liver Disease Severity in Mice and Humans. *Gastroenterology* 134.

6. Pepe-Mooney, B. J., M. T. Dill, A. Alemany, J. Ordovas-Montanes, Y. Matsushita, A. Rao, A. Sen, M. Miyazaki, S. Anakk, P. A. Dawson, N. Ono, A. K. Shalek, A. van Oudenaarden, and F. D. Camargo. 2019. Single-Cell Analysis of the Liver Epithelium Reveals Dynamic Heterogeneity and an Essential Role for YAP in Homeostasis and Regeneration. *Cell Stem Cell* 25: 23-38.e8.

7. Planas-Paz, L., T. Sun, M. Pikiolek, N. R. Cochran, S. Bergling, V. Orsini, Z. Yang, F. Sigoillot, J. Jetzer, M. Syed, M. Neri, S. Schuierer, L. Morelli, P. S. Hoppe, W. Schwarzer, C. M. Cobos, J. L. Alford, L. Zhang, R. Cuttat, A. Waldt, N. Carballido-Perrig, F. Nigsch, B. Kinzel, T. B. Nicholson, Y. Yang, X. Mao, L. M. Terracciano, C. Russ, J. S. Reece-Hoyes, C. Gubser Keller, A. W. Sailer, T. Bouwmeester, L. E. Greenbaum, J. J. Lugus, F. Cong, G. McAllister, G. R. Hoffman, G. Roma, and J. S. Tchorz. 2019. YAP, but Not RSPO-LGR4/5, Signaling in Biliary Epithelial Cells Promotes a Ductular Reaction in Response to Liver Injury. *Cell Stem Cell* 25: 39-53.e10.

8. Jessurun, J. 2018. Histopathologic Approach to Cholestatic Diseases of the Liver. *AJSP Rev. Reports* .

9. Boulter, L., O. Govaere, T. G. Bird, S. Radulescu, P. Ramachandran, A. Pellicoro, R. A. Ridgway, S. S. Seo, B.

Spee, N. Van Rooijen, O. J. Sansom, J. P. Iredale, S. Lowell, T. Roskams, and S. J. Forbes. 2012. Macrophage-derived Wnt opposes Notch signaling to specify hepatic progenitor cell fate in chronic liver disease. *Nat. Med.* 18: 572–579.

10. Jörs, S., P. Jeliazkova, M. Ringelhan, J. Thalhammer, S. Dürl, J. Ferrer, M. Sander, M. Heikenwalder, R. M. Schmid, J. T. Siveke, and F. Geisler. 2015. Lineage fate of ductular reactions in liver injury and carcinogenesis. *J. Clin. Invest.* 125: 2445–2457.

11. Russell, J. O., S. Ko, S. P. Monga, and D. Shin. 2019. Notch inhibition promotes differentiation of liver progenitor cells into hepatocytes via sox9b repression in zebrafish. *Stem Cells Int.* 2019.

12. Huang, M., A. Chang, M. Choi, D. Zhou, F. A. Anania, and C. H. Shin. 2014. Antagonistic interaction between Wnt and Notch activity modulates the regenerative capacity of a zebrafish fibrotic liver model. *Hepatology* 60: 1753–1766.

13. He, J., H. Lu, Q. Zou, and L. Luo. 2014. Regeneration of liver after extreme hepatocyte loss occurs mainly via biliary transdifferentiation in zebrafish. *Gastroenterology* 146.

14. Paku, S., J. Schnur, P. Nagy, and S. S. Thorgeirsson. 2001. Origin and structural evolution of the early proliferating oval cells in rat liver. *Am. J. Pathol.* 158: 1313–1323.

15. Fickert, P., U. Stöger, A. Fuchsbichler, T. Moustafa, H. U. Marschall, A. H. Weiglein, O. Tsybrovskyy, H. Jaeschke, K. Zatloukal, H. Denk, and M. Trauner. 2007. A new xenobiotic-induced mouse model of sclerosing cholangitis and biliary fibrosis. *Am. J. Pathol.* 171: 525–536.

16. Akhurst, B., E. J. Croager, C. A. Farley-Roche, J. K. Ong, M. L. Dumble, B. Knight, and G. C. Yeoh. 2001. A modified choline-deficient, ethionine-supplemented diet protocol effectively induces oval cells in mouse liver. *Hepatology* 34: 519–522.

17. Lu, W. Y., T. G. Bird, L. Boulter, A. Tsuchiya, A. M. Cole, T. Hay, R. V. Guest, D. Wojtacha, T. Y. Man, A. Mackinnon, R. A. Ridgway, T. Kendall, M. J. Williams, T. Jamieson, A. Raven, D. C. Hay, J. P. Iredale, A. R. Clarke, O. J. Sansom, and S. J. Forbes. 2015. Hepatic progenitor cells of biliary origin with liver repopulation capacity. *Nat. Cell Biol.* 17: 973–983.

18. Bird, T. G., M. M ller, L. Boulter, D. F. Vincent, R. A. Ridgway, E. Lopez-Guadamillas, W. Y. Lu, T. Jamieson, O. Govaere, A. D. Campbell, S. Ferreira-Gonzalez, A. M. Cole, T. Hay, K. J. Simpson, W. Clark, A. Hedley, M. Clarke, P. Gentaz, C. Nixon, S. Bryce, C. Kiourtis, J. Sprangers, R. J. Nibbs, N. Van Rooijen, L. Bartholin, S. R. McGreal, U. Apte, S. T. Barry, J. P. Iredale, A. R. Clarke, M. Serrano, T. A. Roskams, O. J. Sansom, and S. J. Forbes. 2018. TGFβ

inhibition restores a regenerative response in acute liver injury by suppressing paracrine senescence. *Sci. Transl. Med.* 10.

19. Español-Suñer, R., R. Carpentier, N. Van Hul, V. Legry, Y. Achouri, S. Cordi, P. Jacquemin, F. Lemaigre, and I. A. Leclercq. 2012. Liver progenitor cells yield functional hepatocytes in response to chronic liver injury in mice. *Gastroenterology* 143.

20. Hofmann, J. J., A. C. Zovein, H. Koh, F. Radtke, G. Weinmaster, and M. L. Iruela-Arispe. 2010. Jagged1 in the portal vein mesenchyme regulates intrahepatic bile duct development: Insights into Alagille syndrome. *Development* 137: 4061–4072.

21. Zong, Y., A. Panikkar, J. Xu, A. Antoniou, P. Raynaud, F. Lemaigre, and B. Z. Stanger. 2009. Notch signaling controls liver development by regulating biliary differentiation. *Development* 136: 1727–1739.

22. Aimaiti, Y., X. Jin, Y. Shao, W. Wang, and D. Li. 2019. Hepatic stellate cells regulate hepatic progenitor cells differentiation via the TGF-β1/Jagged1 signaling axis. *J. Cell. Physiol.* 234: 9283–9296.

23. Mao, Y., S. Tang, L. Yang, and K. Li. 2018. Inhibition of the notch signaling pathway reduces the differentiation of hepatic progenitor cells into cholangiocytes in Biliary Atresia. *Cell. Physiol. Biochem.* 49: 1115–1123.

24. Duncan, A. W., F. M. Rattis, L. N. DiMascio, K. L. Congdon, G. Pazianos, C. Zhao, K. Yoon, J. M. Cook, K. Willert, N. Gaiano, and T. Reya. 2005. Integration of Notch and Wnt signaling in hematopoietic stem cell maintenance. *Nat. Immunol.* 6: 314–322.

25. Demitrack, E. S., G. B. Gifford, T. M. Keeley, N. Horita, A. Todisco, D. Kim Turgeon, C. W. Siebel, and L. C. Samuelson. 2017. NOTCH1 and NOTCH2 regulate epithelial cell proliferation in mouse and human gastric corpus. *Am. J. Physiol. - Gastrointest. Liver Physiol.* 312: G133–G144.

26. Nowotschin, S., P. Xenopoulos, N. Schrode, and A. K. Hadjantonakis. 2013. A bright single-cell resolution live imaging reporter of Notch signaling in the mouse. *BMC Dev. Biol.* 13.

27. Russell, J. O., W. Y. Lu, H. Okabe, M. Abrams, M. Oertel, M. Poddar, S. Singh, S. J. Forbes, and S. P. Monga. 2019. Hepatocyte-Specific β-Catenin Deletion During Severe Liver Injury Provokes Cholangiocytes to Differentiate Into Hepatocytes. *Hepatology* 69: 742–759.

28. Lesaffer, Verboven, Van Huffel, Moya, van Grunsven, Leclercq, Lemaigre, and Halder. 2019. Comparison of the Opn-CreER and Ck19-CreER Drivers in Bile Ducts of Normal and Injured Mouse Livers. *Cells* 8: 380.

29. Chablais, F., and A. Jaźwińska. 2010. IGF signaling between blastema and wound epidermis is required for fin regeneration. *Development* 137: 871–879.

30. Van Landeghem, L., M. A. Santoro, A. T. Mah, A. E. Krebs, J. J. Dehmer, K. K. McNaughton, M. A. Helmrath, S. T. Magness, and P. K. Lund. 2015. IGF1 stimulates crypt expansion via differential activation of 2 intestinal stem cell populations. *FASEB J.* 29: 2828–2842.

31. Osuka, S., O. Sampetrean, T. Shimizu, I. Saga, N. Onishi, E. Sugihara, J. Okubo, S. Fujita, S. Takano, A. Matsumura, and H. Saya. 2013. IGF1 receptor signaling regulates adaptive radioprotection in glioma stem cells. *Stem Cells* 31: 627–640.

32. Van Es, J. H., M. E. Van Gijn, O. Riccio, M. Van Den Born, M. Vooijs, H. Begthel, M. Cozijnsen, S. Robine, D. J. Winton, F. Radtke, and H. Clevers. 2005. Notch/γ-secretase inhibition turns proliferative cells in intestinal crypts and adenomas into goblet cells. *Nature* 435: 959–963.

33. Schouwey, K., I. T. Aydin, F. Radtke, and F. Beermann. 2011. RBP-Jκ-dependent Notch signaling enhances retinal pigment epithelial cell proliferation in transgenic mice. *Oncogene* 30: 313–322.

34. Andersson, E. R., I. V. Chivukula, S. Hankeova, M. Sjöqvist, Y. L. Tsoi, D. Ramsköld, J. Masek, A. Elmansuri, A. Hoogendoorn, E. Vazquez, H. Storvall, J. Netušilová, M. Huch, B. Fischler, E. Ellis, A. Contreras, A. Nemeth, K. C. Chien, H. Clevers, R. Sandberg, V. Bryja, and U. Lendahl. 2018. Mouse Model of Alagille Syndrome and Mechanisms of Jagged1 Missense Mutations. *Gastroenterology* 154: 1080–1095.

35. Gatto, M., V. Drudi-Metalli, A. Torrice, G. Alpini, A. Cantafora, I. Blotta, and D. Alvaro. 2008. Insulin-like growth factor-1 isoforms in rat hepatocytes and cholangiocytes and their involvement in protection against cholestatic injury. *Lab. Investig.* 88: 986–994.

36. Sparks, E. E., D. S. Perrien, K. A. Huppert, T. E. Peterson, and S. S. Huppert. 2011. Defects in hepatic Notch signaling result in disruption of the communicating intrahepatic bile duct network in mice. *DMM Dis. Model. Mech.* 4: 359–367.

37. Dickson, I. 2017. Cholangiocytes regenerate hepatocytes during severe liver injury. *Nat. Rev. Gastroenterol. Hepatol.* 14: 503.

38. Alison, M. R. 2017. Cholangiocytes: No Longer Cinderellas to the Hepatic Regenerative Response. *Cell Stem Cell* 21: 159–160.

39. Lorenzini, S., T. G. Bird, L. Boulter, C. Bellamy, K. Samuel, R. Aucott, E. Clayton, P. Andreone, M. Bernardi, M. Golding, M. R. Alison, J. P. Iredale, and S. J. Forbes. 2010. Characterisation of a stereotypical cellular and extracellular adult liver progenitor cell niche in rodents and diseased human liver. *Gut* 59: 645–654.

40. Knight, B., V. B. Matthews, B. Akhurst, E. J. Croager, E. Klinken, L. J. Abraham, J. K. Olynyk, and G. Yeoh. 2005.

Liver inflammation and cytokine production, but not acute phase protein synthesis, accompany the adult liver progenitor (oval) cell response to chronic liver injury. *Immunol. Cell Biol.* 83: 364–374.

41. Carpino, G., L. Nevi, D. Overi, V. Cardinale, W. Y. Lu, S. Di Matteo, S. Safarikia, P. B. Berloco, R. Venere, P. Onori, A. Franchitto, S. J. Forbes, D. Alvaro, and E. Gaudio. 2020. Peribiliary Gland Niche Participates in Biliary Tree Regeneration in Mouse and in Human Primary Sclerosing Cholangitis. *Hepatology* 71: 972–989.

42. Nguyen, L. N., M. H. Furuya, L. A. Wolfraim, A. P. Nguyen, M. S. Holdren, J. S. Campbell, B. Knight, G. C. T. Yeoh, N. Fausto, and W. T. Parks. 2007. Transforming growth factor-beta differentially regulates oval cell and hepatocyte proliferation. *Hepatology* 45: 31–41.

43. Bird, T. G., W. Y. Lu, L. Boulter, S. Gordon-Keylock, R. A. Ridgway, M. J. Williams, J. Taube, J. A. Thomas, D. Wojtacha, A. Gambardella, O. J. Sansom, J. P. Iredale, and S. J. Forbes. 2013. Bone marrow injection stimulates hepatic ductular reactions in the absence of injury via macrophage-mediated TWEAK signaling. *Proc. Natl. Acad. Sci. U. S. A.* 110: 6542–6547.

44. Guest, R. V., L. Boulter, B. J. Dwyer, T. J. Kendall, T.-Y. Man, S. E. Minnis-Lyons, W.-Y. Lu, A. J. Robson, S. F. Gonzalez, A. Raven, D. Wojtacha, J. P. Morton, M. Komuta, T. Roskams, S. J. Wigmore, O. J. Sansom, and S. J. Forbes. 2016. Notch3 drives development and progression of cholangiocarcinoma. *Proc. Natl. Acad. Sci.* 113: 12250–12255.

45. Zender, S., I. Nickeleit, T. Wuestefeld, I. Sörensen, D. Dauch, P. Bozko, M. El-Khatib, R. Geffers, H. Bektas, M. P. Manns, A. Gossler, L. Wilkens, R. Plentz, L. Zender, and N. P. Malek. 2013. A critical role for notch signaling in the formation of cholangiocellular carcinomas. *Cancer Cell* 23: 784–795.

46. Aloia, L., M. A. McKie, G. Vernaz, L. Cordero-Espinoza, N. Aleksieva, J. van den Ameele, F. Antonica, B. Font-Cunill, A. Raven, R. Aiese Cigliano, G. Belenguer, R. L. Mort, A. H. Brand, M. Zernicka-Goetz, S. J. Forbes, E. A. Miska, and M. Huch. 2019. Epigenetic remodelling licences adult cholangiocytes for organoid formation and liver regeneration. *Nat. Cell Biol.* 21: 1321–1333.

47. Li, W., L. Yang, Q. He, C. Hu, L. Zhu, X. Ma, X. Ma, S. Bao, L. Li, Y. Chen, X. Deng, X. Zhang, J. Cen, L. Zhang, Z. Wang, W. F. Xie, H. Li, Y. Li, and L. Hui. 2019. A Homeostatic Arid1a-Dependent Permissive Chromatin State Licenses Hepatocyte Responsiveness to Liver-Injury-Associated YAP Signaling. *Cell Stem Cell* 25: 54-68.e5.

Acknowledgements: SML is funded by a personal Medical Research Council (MRC) Clinical Fellowship. LB is funded by the The AMMF and the Wellcome Trust (207793/Z/17/Z) and Cancer Research UK (C52499/A27948). RVG is funded by a personal Wellcome Trust fellowship. JM, W-YL, BD and SJF are funded by the MRC (MR/K017047/1) and UK Regenerative Medicine Platform (MR/M007588/1). FL is supported by the Fondation contre le Cancer (2014-125), by the Interuniversity Attraction Pole Programme (Belgian Science Policy, PVII-47) and the FRS-FNRS (Belgium; T.0072.14). NVH and IL are funded by the Fund for Scientific Medical Research (FRS-FNRS, Belgium); the Fondation contre le Cancer (PDR T.1067.14-P and C/2014/207); the Belgian Federal Science Policy Office (Interuniversity Attraction Poles program, network P7/83-HEPRO2). CRUK and the European Research Council fund OJS and TJ.

SML, SFG, NA, TYM, VG, MJW, RVG, WYL, BJD, TJ, CN, NVH generated and analysed data for this study. PLM, JM, IL oversaw and directed the research done in their labs and provided reagents and resources to complete this study. OJS contributed to experimental design and project direction. LB analysed data, directed the project, contributed to experimental design, generated the figures and wrote the manuscript, SJF directed the project, provided funding for the project contributed to experimental design, manuscript writing and manuscript editing.

The BMOL cell line was provided by George Yeoh University of Western Australia. The CK19 antibody Troma-III, developed by Rolf Kemler, was obtained from the Developmental Studies Hybridoma Bank, created by the NICHD of the NIH and maintained at The University of Iowa.

All data presented in this manuscript is available from the authors on request and all tissues, samples and transgenic lines can be made available.

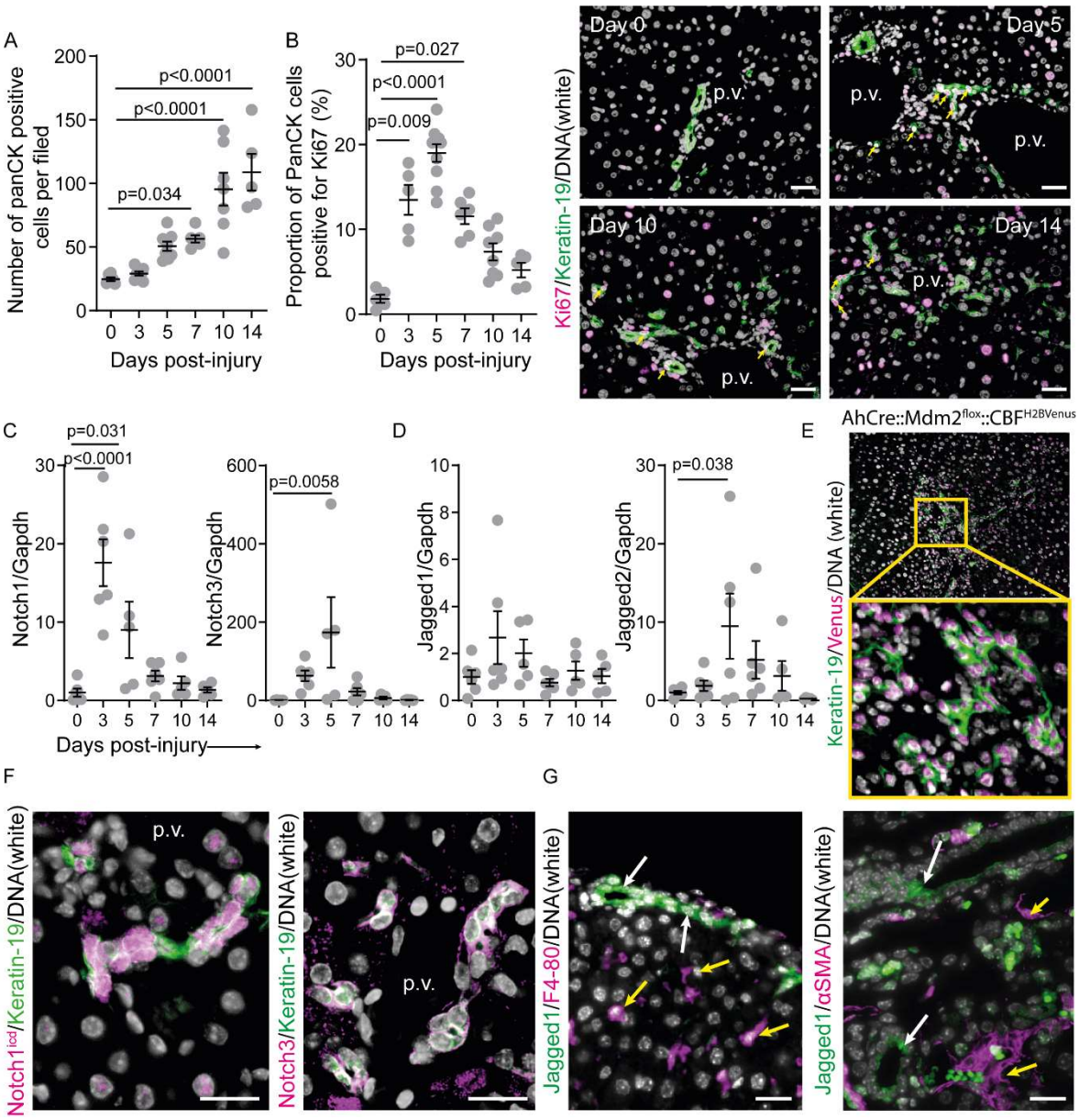
A
Number of panCK positive cells per filed
p<0.0001
p<0.0001
p=0.034
Days post-injury
B
Proportion of PanCK cells positive for Ki67 (%)
p=0.027
p<0.0001
p=0.009
Days post-injury
Ki67/Keratin-19/DNA(white)
Day 0
Day 5
Day 10
Day 14
p.v.
C
Notch1/Gapdh
p=0.031
p<0.0001
Notch3/Gapdh
p=0.0058
Days post-injury
D
Jagged1/Gapdh
Jagged2/Gapdh
p=0.038
E
AhCre::Mdm2flox::CBFH2BVenus
Keratin-19/Venus/DNA (white)
F
Notch1icd/Keratin-19/DNA(white)
Notch3/Keratin-19/DNA(white)
G
Jagged1/F4-80/DNA(white)
Jagged1/αSMA/DNA(white)

Figure 1: Notch pathway activation precedes BEC proliferation. **A**. Quantification of panCK positive BECs between day 0 (initiation of injury) and d14 following injury and the proportion of panCK positive BECs that are proliferating, immunostained with Ki67. **B**. Immunohistochemistry of panCK positive bile ducts and BECs (green) and Ki67 (red) following initiation of injury. Yellow arrows denote nuclear positivity of Ki67 and white denotes DNA. **C**. mRNA expression of *Notch1* and *Notch3* in whole liver tissue following injury induction. **D.** Notch ligands, *Jagged-1* and *Jagged-2* mRNA expression over the injury time course. **E**. Immunostaining of Ah-Cre::$Mdm2^{fl/fl}$::$CBF^{H2Bvenus}$ mice five days following induction. (Keratin-19, green, Venus (reporting Notch activity), magenta). Yellow box denotes zoomed in region in lower panel. **F**. Immunofluorescent staining of NOTCH1 (3 days following injury) and NOTCH3 (five days following injury), pink, and Keratin-19 (demarcating BECs), left hand panels. **G.** Immunofluorescent staining of the Notch-ligand, JAGGED-1 (green) and either F4-80, αSMA or Keratin-19 (magenta), all five days post-injury. Yellow arrows denote Jagged-1 negative cells. White arrows denote Jagged-1 positive cholangiocytes. In all immunofluorescent staining, DNA is stained white. Scale Bar = 50μm. p.v. denotes portal vein. N=6 per group. Each point represents a biological replicate. Data was analysed using an ANOVA and a Dunnett's multiple comparison test.

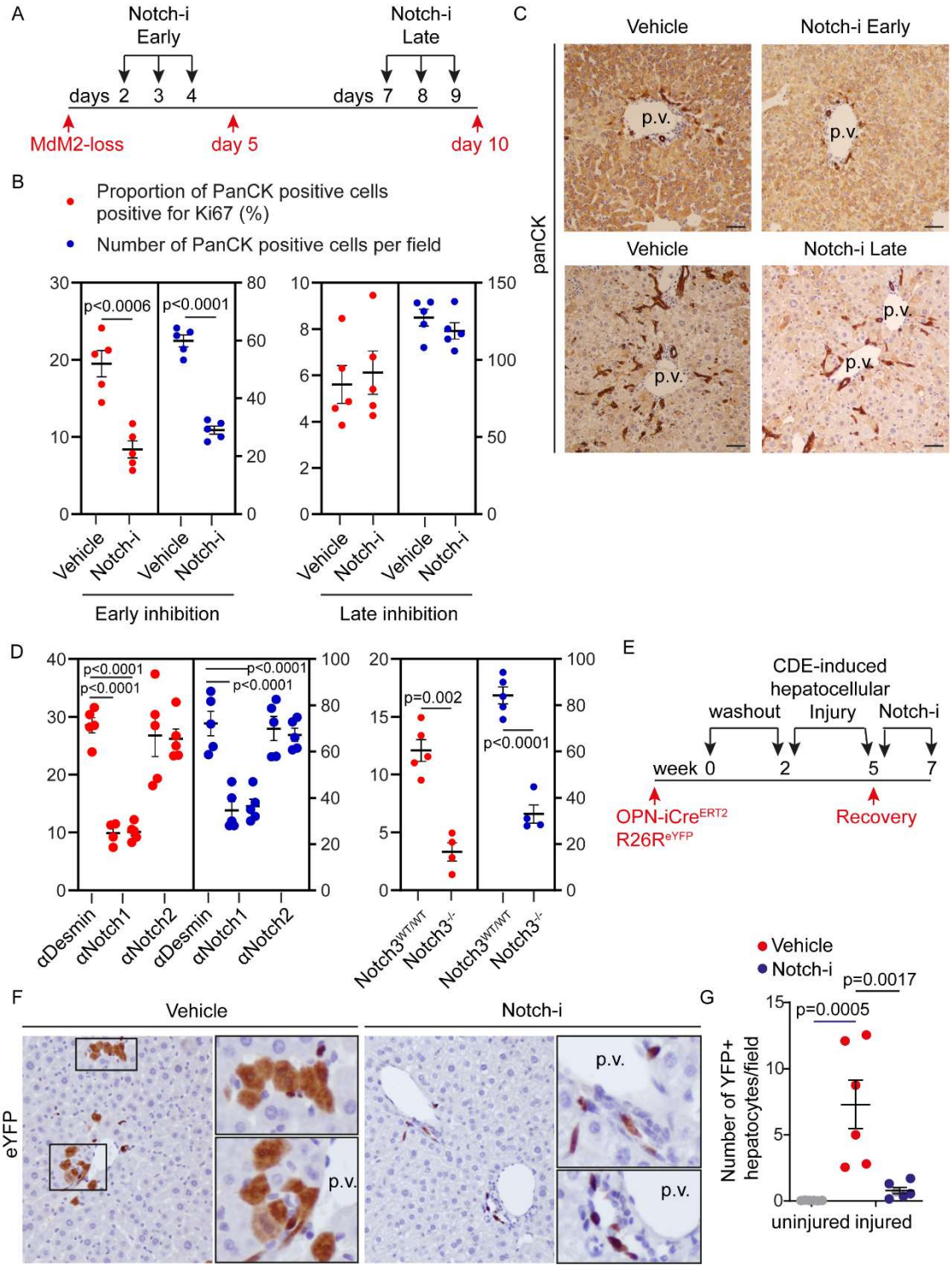
A
Notch-i Early
Notch-i Late
days 2 3 4
days 7 8 9
MdM2-loss
day 5
day 10
B
Proportion of PanCK positive cells positive for Ki67 (%)
Number of PanCK positive cells per field
p<0.0006
p<0.0001
Vehicle
Notch-i
Early inhibition
Late inhibition
C
Vehicle
Notch-i Early
Notch-i Late
panCK
p.v.
D
p<0.0001
p=0.002
αDesmin
αNotch1
αNotch2
Notch3WT/WT
Notch3-/-
E
CDE-induced hepatocellular
washout
Injury
Notch-i
week 0
2
5
7
OPN-iCreERT2
R26ReYFP
Recovery
F
Vehicle
Notch-i
eYFP
G
Vehicle
Notch-i
p=0.0017
p=0.0005
Number of YFP+ hepatocytes/field
uninjured
injured

Figure 2: Inhibition of specific Notch receptors alters BEC proliferation and differentiation in vivo. **A.** Schematic representation of early and late inhibition of Notch signalling during hepatocyte regeneration from BECs in the Mdm2 model. **B.** Quantification of proliferative (Ki67 positive) BECs (red dots) and total number of panCK positive BECs (blue dots) following Notch inhibition with DAPT either early in regeneration (left panel) or late in regeneration (right panel). **C.** Immunohistochemistry for BECs (stained with panCK) following inhibition of Notch signalling with DAPT either early or late following injury. **D.** Quantification of the number of proliferating (Ki67 positive) BECs (red dots) and total number of panCK positive BECs (blue dots) following inhibition with a blocking antibody targeting Desmin (an intermediate filament protein that serves as a control) and receptor specific blocking antibodies targeting either NOTCH1 or NOTCH2 (left panel). Individual groups represent distinct antibody clones. Right panel, proportion of proliferating (Ki67 positive) BECs (red dots) and total number of panCK positive BECs (blue dots) following *Mdm2*-loss induced injury in mice with either wild-type ($Notch3^{WT/WT}$)or null for *Notch3* ($Notch3^{-/-}$). **E.** Schematic representation of lineage tracing BECs into hepatocytes using OPN-$iCre^{ERT2}$::$R26R^{eYFP}$ transgenic mice treated with a Choline Deficient, Ethionine Supplemented (CDE) diet. **F.** Immunohistochemistry showing eYFP positive cells during hepatic repair in control and Notch-i treated mice. **G.** Quantification of the number of eYFP (lineage-traced) hepatocytes following Notch-i treatment. Scale Bar = 50µm. p.v. denotes portal vein. N≥4 per group. Each point represents a biological replicate. For data with two groups, a Student's t-test was performed where multiple groups are analysed an ANOVA and a Dunnett's multiple comparison test were used.

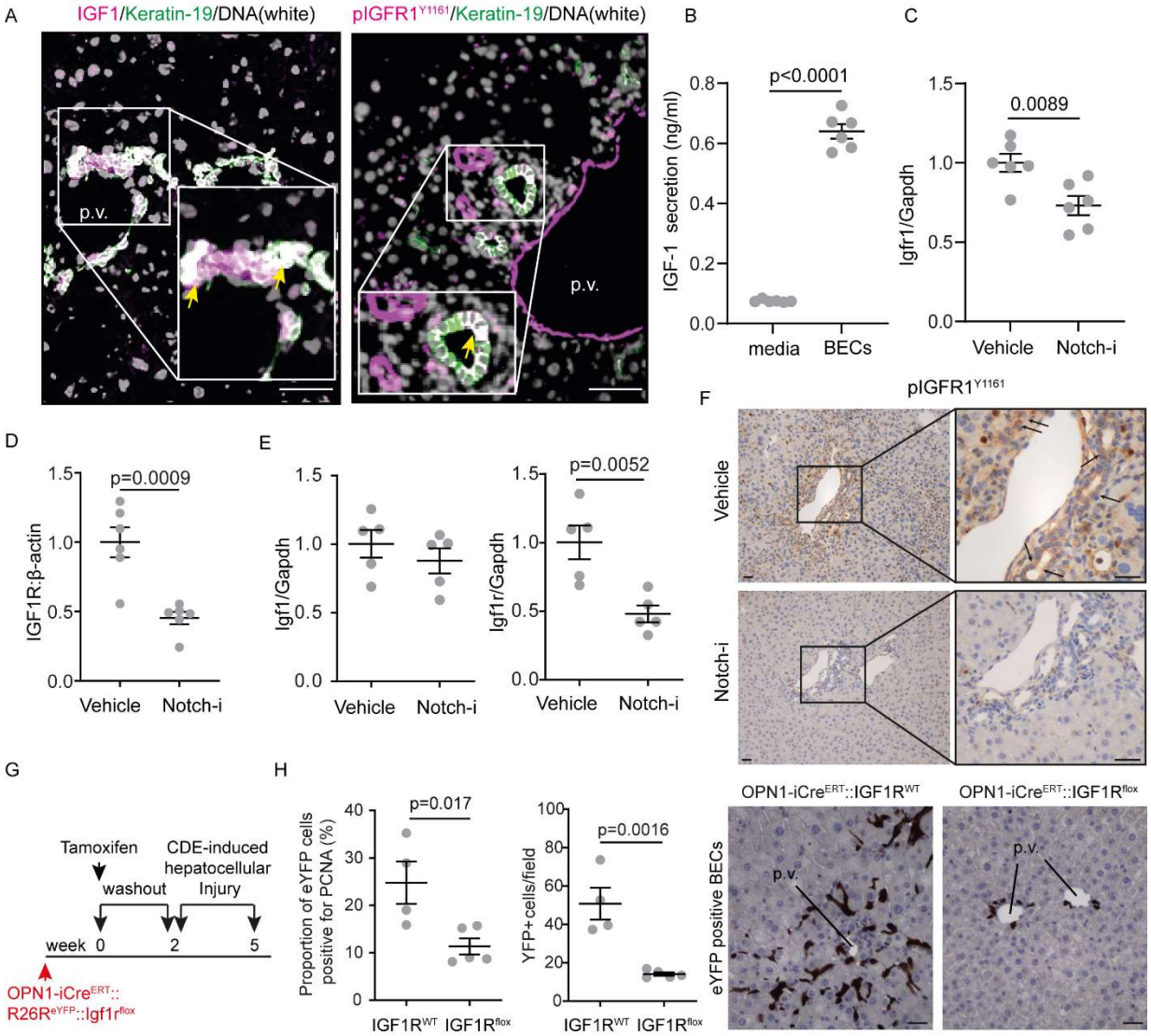
A
IGF1/Keratin-19/DNA(white)
pIGFR1Y1161/Keratin-19/DNA(white)
p.v.
p.v.
B
p<0.0001
IGF-1 secretion (ng/ml)
media
BECs
C
0.0089
Igfr1/Gapdh
Vehicle
Notch-i
D
p=0.0009
IGF1R:β-actin
Vehicle
Notch-i
E
Igf1/Gapdh
Igf1r/Gapdh
p=0.0052
F
pIGFR1Y1161
Vehicle
Notch-i
G
Tamoxifen
washout
CDE-induced hepatocellular Injury
week 0
2
5
OPN1-iCreERT::
R26ReYFP::Igf1rflox
H
p=0.017
Proportion of eYFP cells positive for PCNA (%)
IGF1RWT
IGF1Rflox
p=0.0016
YFP+cells/field
OPN1-iCreERT::IGF1RWT
OPN1-iCreERT::IGF1Rflox
eYFP positive BECs
p.v.
p.v.

Figure 3: Notch signalling regulates IGFR1 expression in BECs, to regulate their proliferation. **A.** Immunofluorescent staining of IGF1 (pink) in BECs (stained with Keratin-19, green), left panel and phosphorylated $IGF1R^{Y1161}$ (pink) in BECs (green), right panel at day 7 following injury. DNA is in white. Yellow arrows denote co-positivity. Inset images represent area of interest at an increased magnification. **B.** ELISA for IGF-1 secreted into the media by the BMOL BEC cell lines. **C.** mRNA expression of *Igfr1* in BECs treated with vehicle or Notch-i, DAPT in vitro. **D.** Protein levels of total IGF1R normalised to β-actin levels following Notch-i treatment. **E.** mRNA expression of IGF1 and IGF1R in liver tissue undergoing hepatocyte regeneration treated with vehicle or Notch-i, DAPT. **F.** Immunohistochemical staining for phosphorylated $IGF1R^{Y1161}$ in animals undergoing hepatocyte regeneration treated with either vehicle or Notch-i. Black arrows denote membrane staining. **G.** Schematic detailing the strategy to delete *Igf1r* in BECs using the OPN-$iCre^{ERT}$ combined with an $Igf1^{flox}$ allele treated and with CDE to induce hepatocyte injury, regeneration and BEC proliferation. **H.** Proportion of eYFP positive BECs that are proliferative, determined through co-positivity with PCNA (left dot plot) and total number of BECs following loss of IGF1R (right dot plot). Immunohistochemistry panels show representative eYFP staining (brown) of BECs in $IGF1R^{WT}$ and $IGF1R^{flox}$ mice at week five. Scale Bar = 50μm. p.v. denotes portal vein. N=6 per group. Each point represents a biological replicate. For data with two experimental groups, a Student's t-test was used to determine significance.

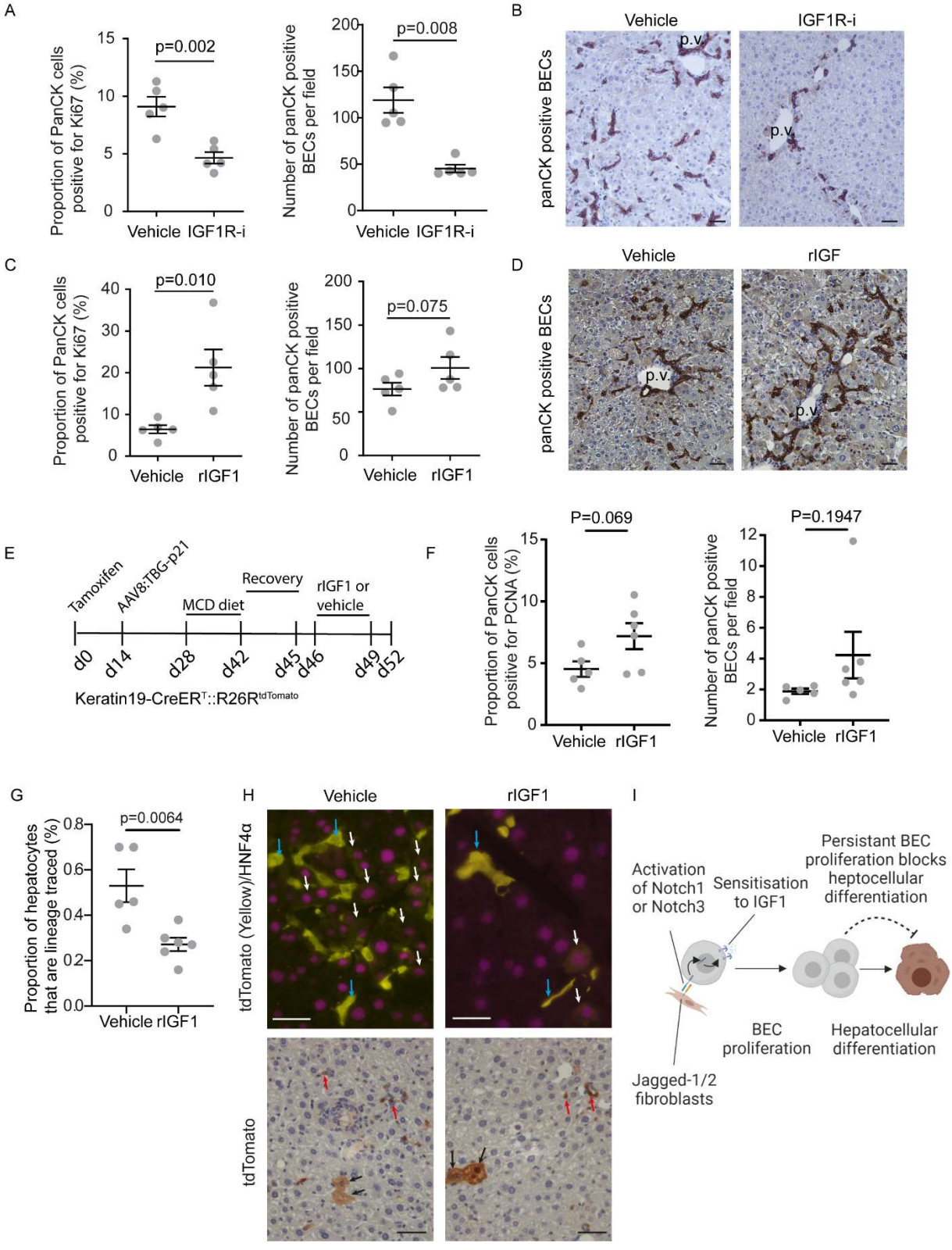
A
Proportion of PanCK cells positive for Ki67 (%)
p=0.002
Vehicle IGF1R-i
Number of panCK positive BECs per field
p=0.008
Vehicle IGF1R-i
B
Vehicle
IGF1R-i
panCK positive BECs
p.v.
C
Proportion of PanCK cells positive for Ki67 (%)
p=0.010
Vehicle rIGF1
Number of panCK positive BECs per field
p=0.075
Vehicle rIGF1
D
Vehicle
rIGF
panCK positive BECs
p.v.
E
Tamoxifen
AAV8:TBG-p21
MCD diet
Recovery
rIGF1 or vehicle
d0 d14 d28 d42 d45 d46 d49 d52
Keratin19-CreER^{T}::R26R^{tdTomato}
F
Proportion of PanCK cells positive for PCNA (%)
P=0.069
Vehicle rIGF1
Number of panCK positive BECs per field
P=0.1947
Vehicle rIGF1
G
Proportion of hepatocytes that are lineage traced (%)
p=0.0064
Vehicle rIGF1
H
Vehicle
rIGF1
tdTomato (Yellow)/HNF4α
tdTomato
I
Activation of Notch1 or Notch3
Sensitisation to IGF1
Persistant BEC proliferation blocks heptocellular differentiation
BEC proliferation
Hepatocellular differentiation
Jagged-1/2 fibroblasts

Figure 4: Therapeutic IGF1R modulation regulates BEC number in vivo but does not promote reconstitution of the parenchyma. **A.** Proportion of Ki67 (proliferative) BECs (left dot plot) and total number of BECs (right dot plot) in vehicle treated or IGF1R-inhibitor (AG1024) treated mice, and **B** immunohistochemistry showing panCK-positive BECs following hepatocyte Mdm2-loss and treatment with IGF1R-inhibitor or vehicle alone. **C.** Proportion of Ki67 (proliferative) BECs (left dot plot) and total number of BECs (right dot plot) in vehicle treated or rIGF1 treated mice, and **D.** immunohistochemistry showing panCK-positive BECs following hepatocyte *Mdm2*-loss and treatment with rIGF1 or vehicle alone. **E.** Schematic detailing the approach taken to determine whether rIGF1-induced BEC expansion results in the formation of more parenchymal hepatocytes. **F.** Proportion of PCNA-positive (proliferative) BECs (left dot plot) and total number of BECs (right dot plot) in vehicle treated or rIGF1 treated mice following injury. **G.** Proportion of HNF4α positive hepatocytes that are also positive for tdTomato (lineage traced) in vehicle and rIGF1 treated animals having received hepatocyte injury with MCD and **H.** Immunofluorescence of tdTomato (yellow) and HNF4α (magenta) at day 52 following MCD injury and rIGF1 treatment. Blue arrows denote tdTomato positive BECs and white arrows denote tdTomato positive, lineage traced hepatocytes. Lower panels demonstrate tdTomato positive hepatocytes detected with DAB (black arrows), red arrows denote tdtomato positive BECs. **I.** Diagram showing our model, in which Notch signalling promotes BEC proliferation by rIGF1, yet differentiation into hepatocytes is not increased. Scale Bar = 50μm. p.v. denotes portal vein. N≥3 per group. Each point represents a biological replicate. For data with two experimental groups, a Student's t-test was used to determine significance.

Supplementary Material:

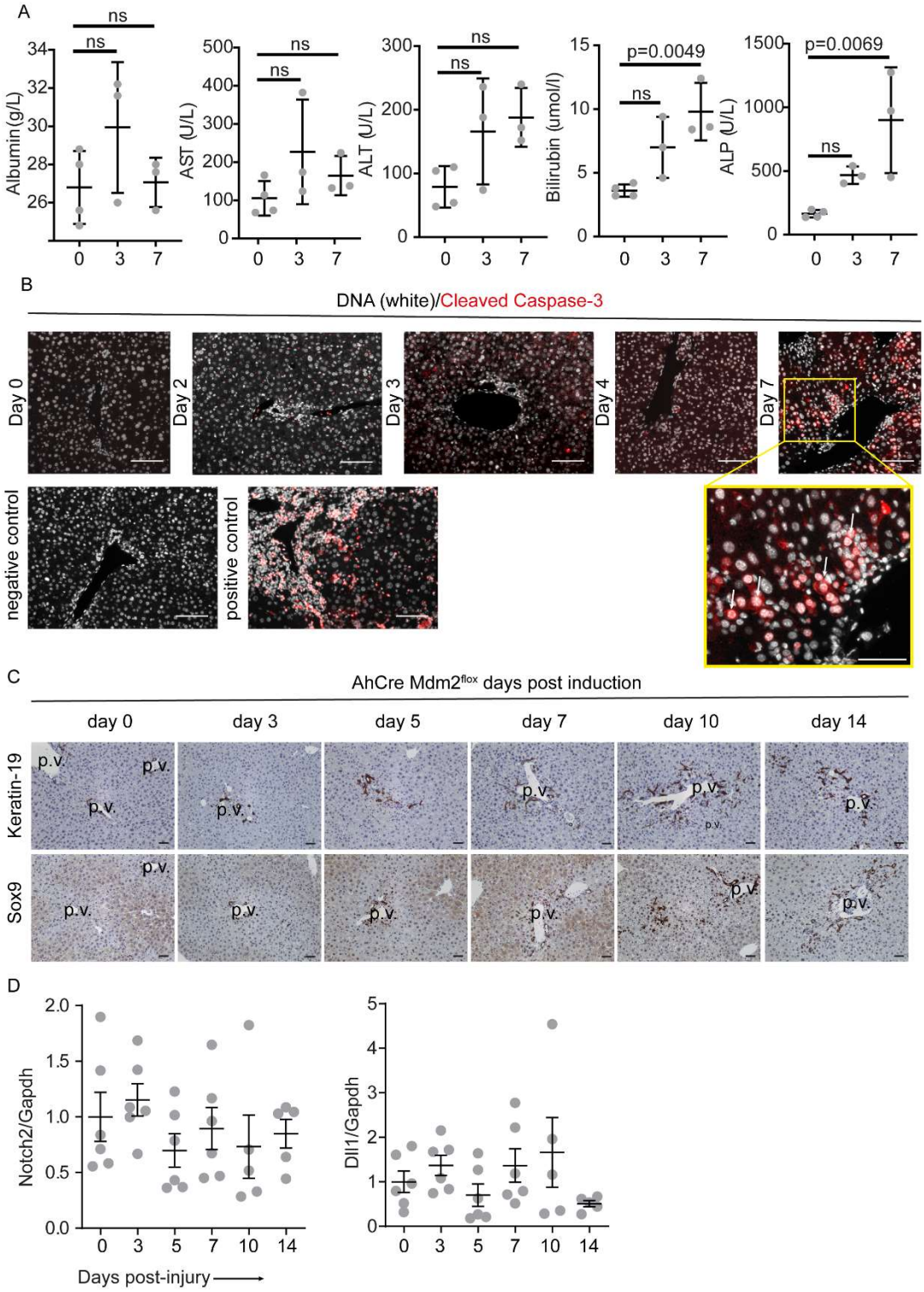

Supplementary Figure 1: Deletion of Mdm2 in hepatocytes induced apoptosis and induces BECs to proliferate. **A.** Blood serum biochemistry for liver function at baseline (d0) and d3 and d7 following *Mdm2* inactivation. **B.** Immunohistochemistry showing positivity for cleaved Caspase-3 (red) following inactivation of *Mdm2* in hepatocytes. DNA is shown in white. Yellow box denotes region of high magnification image, inset. White arrows denote Caspase-3 positive hepatocytes. **C.** Immunohistochemical staining of BECs using the markers Keratin-19 (upper panels) and SOX9 (lower panels) following hepatocyte loss of *Mdm2*. **D.** mRNA expression following the recombination of *Mdm2* in hepatocytes, for *Notch2* and *Dll1*, a Notch receptor ligand. mRNA expression is normalised to the housekeeping gene *Gapdh*. *Notch4* and *Dll3* and *Dll4* were not detectable by qRT-PCR. Scale bar = 50µm. N=4-6 per group. Each point represents a biological replicate. For data with two groups, a Student's t-test was performed where multiple groups are analysed an ANOVA and a Dunnett's multiple comparison test were used.

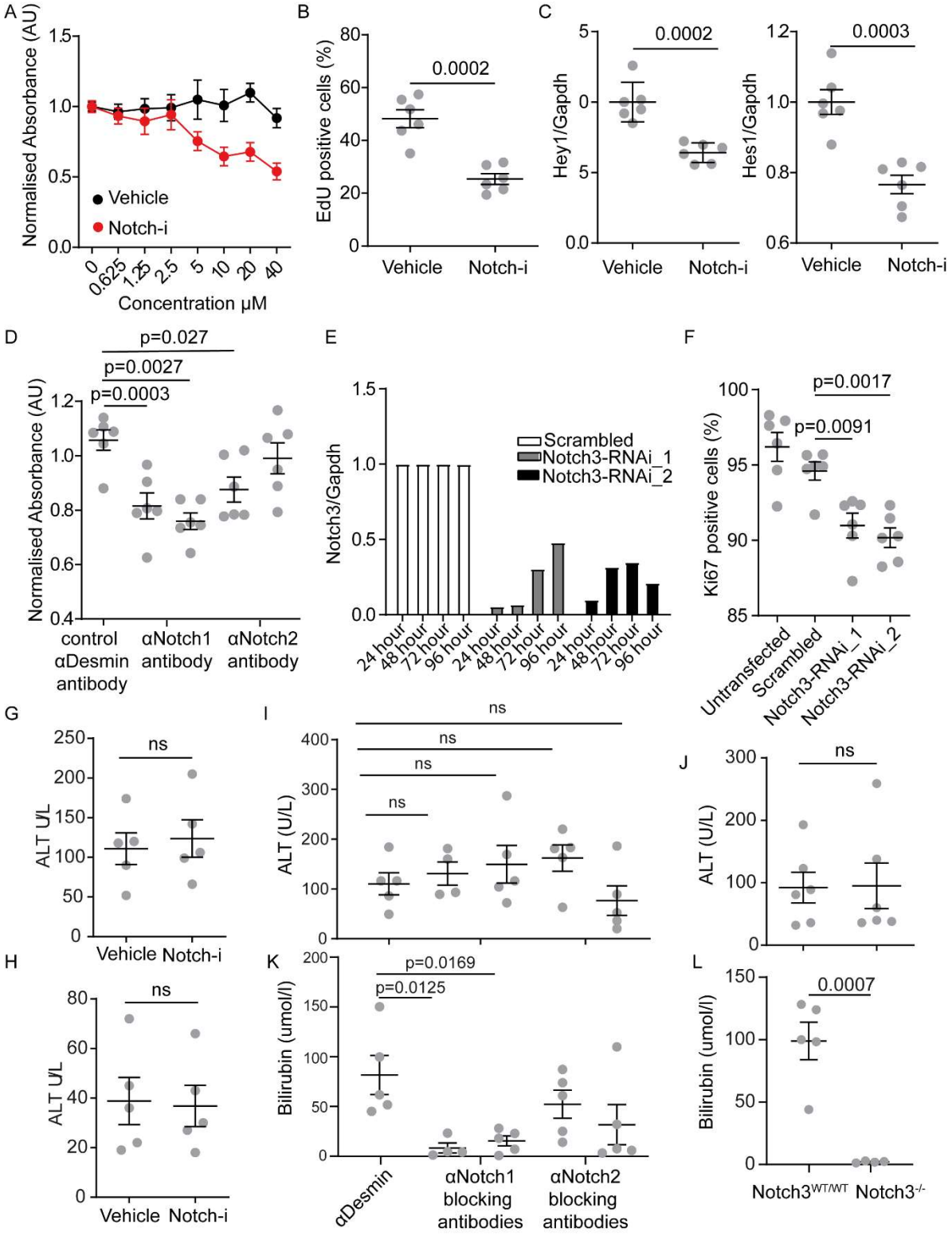
A
Normalised Absorbance (AU)
Vehicle
Notch-i
Concentration µM
B
EdU positive cells (%)
0.0002
Vehicle
Notch-i
C
Hey1/Gapdh
0.0002
Hes1/Gapdh
0.0003
D
p=0.027
p=0.0027
p=0.0003
Normalised Absorbance (AU)
control αDesmin antibody
αNotch1 antibody
αNotch2 antibody
E
Notch3/Gapdh
Scrambled
Notch3-RNAi_1
Notch3-RNAi_2
24 hour
48 hour
72 hour
96 hour
F
Ki67 positive cells (%)
p=0.0017
p=0.0091
Untransfected
Scrambled
Notch3-RNAi_1
Notch3-RNAi_2
G
ALT U/L
ns
Vehicle
Notch-i
H
ALT U/L
ns
Vehicle
Notch-i
I
ALT (U/L)
ns
J
ALT (U/L)
ns
K
Bilirubin (umol/l)
p=0.0169
p=0.0125
αDesmin
αNotch1 blocking antibodies
αNotch2 blocking antibodies
L
Bilirubin (umol/l)
0.0007
Notch3WT/WT
Notch3-/-

Supplementary Figure 2: In vitro inhibition of Notch signalling reduces BEC proliferation. **A.** MTT assay showing the response of BECs in vitro when treated with a scaling dose of Notch-i, DAPT or vehicle alone. **B.** The number of Edu-positive (proliferating) BECs in vitro when treated with the Notch-i, DAPT or vehicle alone. **C.** mRNA expression of Notch pathway target genes *Hey1* and *Hes1* following Notch pathway inhibition. **D.** MTT assay of BECs following treatment with a control blocking antibody targeting the intermediate filament protein, Desmin or targeting either NOTCH1 or NOTCH2 specifically. Individual groups represent distinct antibody clones. **E.** mRNA expression of *Notch3* in BECs in vitro following treatment with two RNAi targeting *Notch3* normalised to cells treated with a scrambled RNAi. **F.** Number of Ki67 positive BECs in vitro following knock-down of Notch3 compared to untransfected and scrambled RNAi transfected cells. **G.** Blood serum biochemistry for ALT following *Mdm2* inactivation and early (days 2-4) treatment with the Notch-i, DAPT **H**. Blood serum biochemistry for ALT following *Mdm2* inactivation and late (days 7-9) treatment with the Notch-i, DAPT. **I.** Blood serum biochemistry for ALT following *Mdm2* inactivation and treatment with either NOTCH-1, NOTCH-2 or Desmin (an intermediate filament protein that acts as a control) blocking antibodies. **J.** Blood serum biochemistry for ALT following *Mdm2* inactivation in mice harboring wild-type *Notch3* or null for *Notch3* (Notch3-/-). **K.** Blood serum biochemistry for Bilirubin following *Mdm2* inactivation and treatment with either NOTCH-1, NOTCH-2 or Desmin (an intermediate filament protein that acts as a control) blocking antibodies. **L.** Blood serum biochemistry for Bilirubin following *Mdm2* inactivation in mice harboring wild-type *Notch3* or null for *Notch3* (Notch3-/-). N=4-6 per group. Each point represents a biological or experimental replicate. For data with two groups, a Student's t-test was performed where multiple groups are analysed an ANOVA and a Dunnett's multiple comparison test were used.

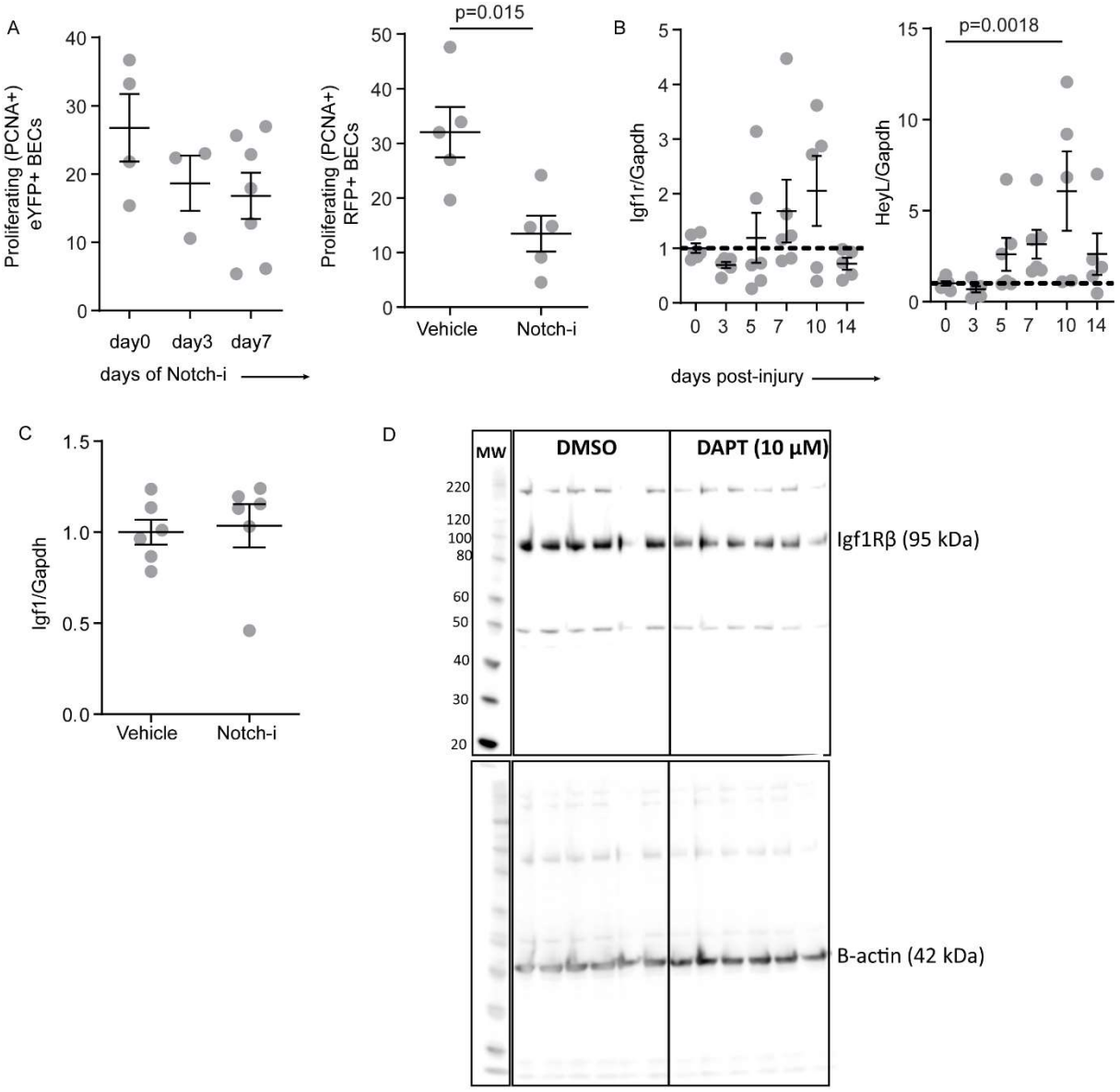
A
Proliferating (PCNA+) eYFP+ BECs
day0
day3
day7
days of Notch-i
Proliferating (PCNA+) RFP+ BECs
p=0.015
Vehicle
Notch-i
B
Igf1r/Gapdh
days post-injury
HeyL/Gapdh
p=0.0018
C
Igf1/Gapdh
Vehicle
Notch-i
D
MW
DMSO
DAPT (10 µM)
Igf1Rβ (95 kDa)
B-actin (42 kDa)

Supplementary Figure 3: Notch signalling regulates IGF1 sensitivity by regulating IGF1R activity. **A.** Dot plots showing that the Notch-i, DAPT reduces proliferation of BECs in the Choline Deficient Ethionine-Supplemented (CDE), left graph, and Methionine-Choline Deficient, MCD diet, right graph. **B.** mRNA expression of *Igf1* in pBECs following treatment with the Notch-i, DAPT. **C.** mRNA expression of *Igf1R* and the Notch target gene, *HeyL* in whole liver tissue following induction of hepatic injury. **D.** Protein expression of IGF1R in vehicle treated pHPCs, compared to pHPCs treated with Notch-i, DAPT. N≥5 per group. Each point represents a biological replicate. For data with two groups, a Student's t-test was performed where multiple groups are analysed an ANOVA and a Dunnett's multiple comparison test were used.

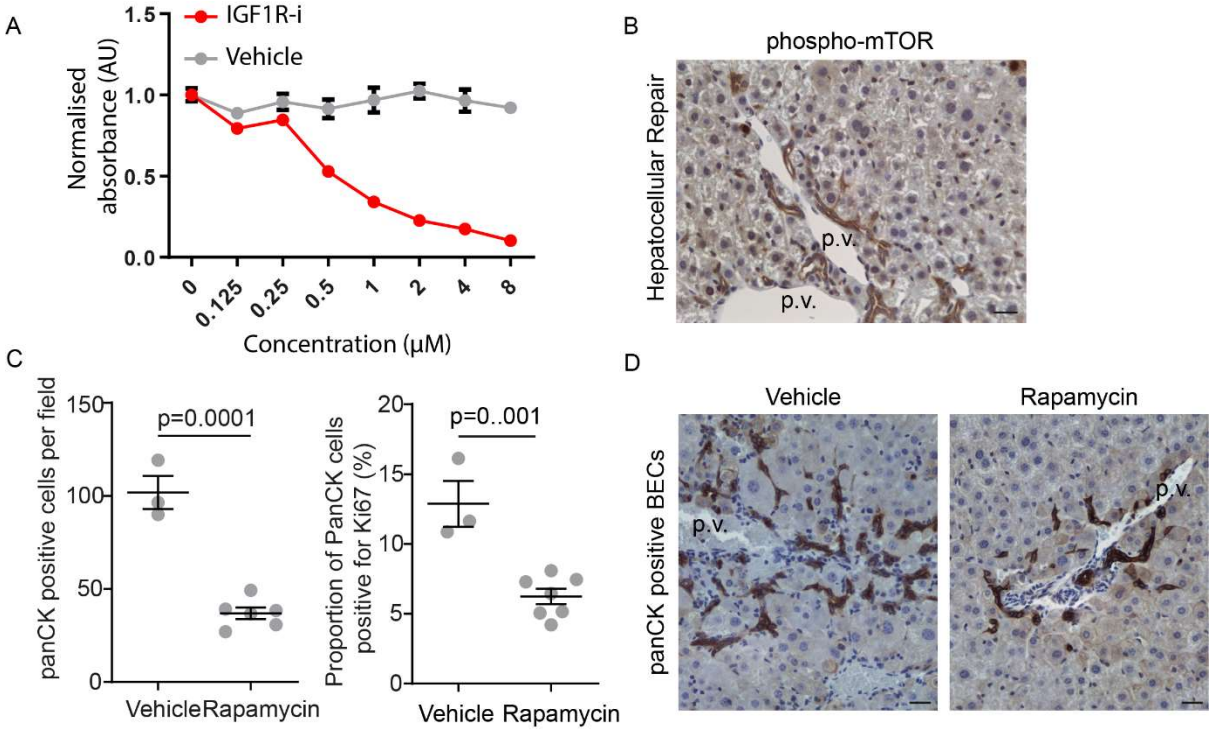
A
IGF1R-i
Vehicle
Normalised absorbance (AU)
1.5
1.0
0.5
0.0
0
0.125
0.25
0.5
1
2
4
8
Concentration (μM)
B
phospho-mTOR
Hepatocellular Repair
p.v.
p.v.
C
panCK positive cells per field
150
100
50
0
p=0.0001
Vehicle
Rapamycin
Proportion of PanCK cells positive for Ki67 (%)
20
15
10
5
0
p=0..001
Vehicle
Rapamycin
D
Vehicle
Rapamycin
panCK positive BECs
p.v.
p.v.

Supplementary Figure 4: mTOR signalling can control BEC proliferation following hepatic injury**. A.** MTT assay of HPC growth with escalating concentrations of AG1024, an IGF1R-i or vehicle alone. **B.** Immunohistochemistry of phosphorylated mTOR in HPCs undergoing hepatocyte regeneration. **C.** Quantification of total Keratin-19 positive BEC number, left graph, and Ki67 positive (proliferating) BECs, right graph, following induction of hepatocyte regeneration and subsequent treatment with the mTOR inhibitor, Rapamycin. **D.** Immunohistochemistry of panCK positive BECs in livers where *Mdm2* has been inactivated and animals have been treated with either vehicle or Rapamycin, images represent animals that were culled at 10 days following initiation of injury and which were treated with Rapamycin or vehicle from days 6-9. N≥3 per group. Each point represents a biological replicate or experimental replicate. Scale bar = 50μm For data with two groups, a Student's t-test was used.

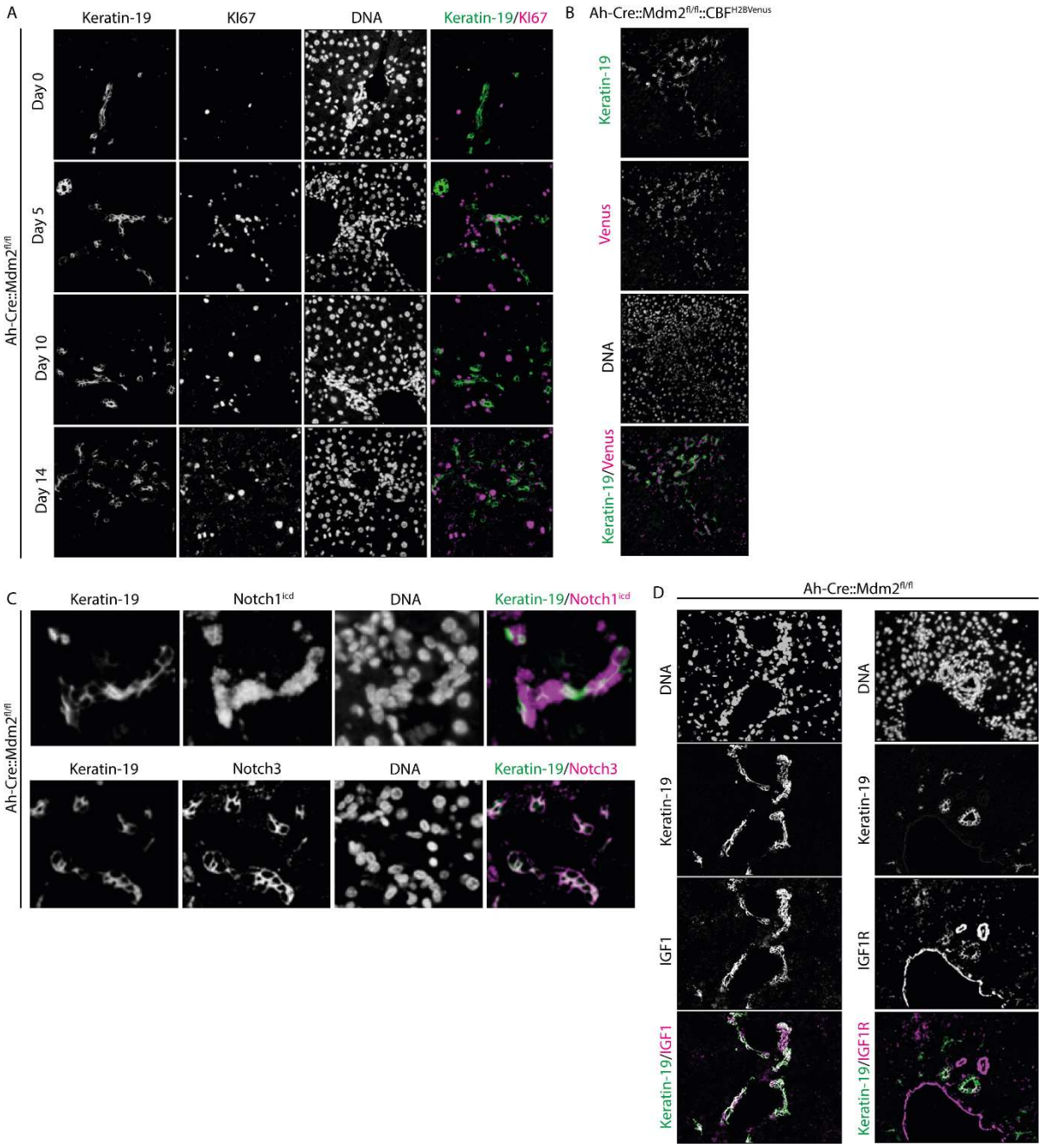
A
Keratin-19
KI67
DNA
Keratin-19/KI67
Ah-Cre::Mdm2fl/fl
Day 0
Day 5
Day 10
Day 14
B
Ah-Cre::Mdm2fl/fl::CBFH2BVenus
Keratin-19
Venus
DNA
Keratin-19/Venus
C
Keratin-19
Notch1icd
DNA
Keratin-19/Notch1icd
Keratin-19
Notch3
DNA
Keratin-19/Notch3
Ah-Cre::Mdm2fl/fl
D
Ah-Cre::Mdm2fl/fl
DNA
Keratin-19
IGF1
Keratin-19/IGF1
DNA
Keratin-19
IGF1R
Keratin-19/IGF1R

Supplementary Figure 5: Single channels of immunofluorescence presented within this study. **A-C.** Single fluorescent channels from Figure 1: Notch pathway activation precedes BEC proliferation. **D** Single fluorescent channels from Figure 3: Notch signalling regulates IGFR1 expression in BECs, to regulate their proliferation.

Supplementary Table 1: Antibodies and Primers used in this study.

Antibodies used in this study		
Caspase-3	Cell Signalling	9662
CK19	Developmental studies hybridoma bank	Troma-III
Hnf4α	R&D systems	H1415
IGF1	Abcam	ab40657
IGF1 receptor β	Cell Signalling Technologies	9750
Jagged-1	Abcam	ab109536
Ki67	Abcam	ab16667
mCherry	Sicgen	#AB0081
Notch1-ICD	Abcam	Ab8925
Notch3	Abcam	Ab23426
panCK	DAKO	Z0622
PCNA	Abcam	ab29
YFP	Abcam	ab6673
Primers used in this study		
Dll1	Qiagen	QT00113239
Dll3	Qiagen	QT00113477
Dll4	Qiagen	QT01053598
Gapdh	Qiagen	QT01658692
Hes1	Qiagen	QT00313537
Hey1	Qiagen	QT00115094
Igf1	Qiagen	QT00154469
Igf1r	Qiagen	QT00155351
Jagged1	Qiagen	QT00115703
Jagged2	Qiagen	QT01043819
Notch1	Qiagen	QT00156982
Notch2	Qiagen	QT00153496
Notch3	Qiagen	QT01051729
Notch4	Qiagen	QT00135653